

**Actively targeted nano-carrier system for the co-delivery Temozolomide
and an autophagy modulator for the treatment of glioblastoma multiforme**



Candidate name: Prabhjeet Singh

Under the supervision of

Dr. Deepak Chitkara

Associate Professor, Department of Pharmacy

BITS-PILANI, Pilani, Rajasthan

Introduction

Glioblastoma (GBM) is the most prevalent and deadly primary malignant brain tumor in adults, accounting for 16 percent of all brain and central nervous system tumors. Regardless of sophisticated diagnostic methods and the finest multimodal treatment, constituting surgical resection, radiotherapy, and concurrent temozolomide chemotherapy, most patients experience nominal progression-free survival and tumor relapse. This could be attributed mainly to tumor heterogeneity, infiltration pattern, and location, rendering it more lethal. The current treatment for GBM includes tumor resection, with concomitant radiation therapy and chemotherapy. Despite intensive treatment, the average survival of GBM-affected patients remains around 50-65 weeks. A small molecule, temozolomide (TMZ), has demonstrated a promising effect in treating malignant gliomas and other hard-to-treat malignancies in conjugation with radiotherapy [1]. Temozolomide (TMZ) is a second-generation DNA alkylating agent used as a standard-of-care chemotherapeutic agent for treating glioblastoma multiforme (GBM). TMZ is marketed as Temodal® in the form of capsules and injectables to be administered orally and intravenously, respectively. Though a potent molecule, TMZ exhibits several limitations such as short half-life, rapid pH-dependent hydrolysis, and quick clearance resulting in lesser accumulation in the brain. Hydrolysis of the molecule under physiological conditions results in the conversion of TMZ into its metabolite MTIC (3-methyl-(triazene-1-yl)imidazole-4-carboxamide) and AIC (5-aminoimidazole-4-carboxamide), which cannot permeate into the cells effectively. Only <1% of the dose reaches the brain intact, thereby rendering the drug with sub-therapeutic outcomes. In order to achieve the therapeutic effect, high doses of TMZ is given, thereby resulting in dose-dependent haematological toxicities. Several approaches have been explored to overcome these limitations, including the encapsulation in nanocarriers of organic (lipids, polymers, dendrimers, etc.) and inorganic (silica, quantum dots, gold, silver, etc.) materials that showed improved TMZ delivery [1] as well as preparation of conjugates with small molecules and polymers. TMZ has a solubility of 5 mg/ml, which poses challenges in encapsulating TMZ in nanocarriers. In the conjugation approach TMZ has been conjugated with small molecules such as doxorubicin, γ -carbolines, 5-nitro-2-(3-phenylpropylamino)-benzoate (NPPB), perillyl Alcohol, etc. and polymer including poly-(2-methacryloyloxyethyl phosphorylcholine) (MPC), poly(β -L-malic acid), poly(2-ethyl-2-oxazoline), etc. TMZ conjugated to the polymeric backbone demonstrated improved drug loading capacity, systemic circulation, tissue targeting, ease in fabrication, and better biocompatibility.

Likewise, a series of polymer-TMZ conjugates depicted an effecting drug loading capacity up to 35-50 mol% with improved stability half-life ranging from 2-19 folds compared to free TMZ. Furthermore, the *in vitro* cell-based assay also depicted marked enhancement in the cytotoxicity and uptake in glioma cell lines [2]. In another study, multifunctional targeted poly(β -L-malic acid) conjugated to TMZ was synthesized, resulting in particles of 6.5-14.8 nm, improved the loading capacity up to 17 %w/w with enhanced stability of TMZ from 1.8 h to 5-7 h [3]. We and others have previously reported the drug conjugates using PEG-polycarbonate, providing ample opportunity to attach the drug to the polycarbonate backbone with improved loading capacity, stability, and efficacy. Though conjugating TMZ with mPEG-polycarbonate overcomes the limitations associated with TMZ, there is still a lot of scope for further improvement. Herein, we report a hybrid system comprising the TMZ nanoconjugates and mPEG-PLA. Combining polymers with polymer-drug conjugates could provide benefits such as improved stability, biomimetic nature, reduced clearance, increased drug accumulation to the target site, and reduced toxicity. Several other hybrid nanosystems have been explored earlier. For instance, polymer-lipid hybrid nanoparticles were prepared using PLGA polymer, and HSPC, DSPC, and cholesterol as a lipid were prepared using the solvent emulsification method. The hybrid lipid-polymer nanosystem exhibited an average particle size of ca. 256 nm with an encapsulation efficiency of >60% at drug loading of ~3% w/w [4]. We have also previously reported polymer-lipid hybrid systems to deliver small molecules. Combining the polymer drug conjugates provide an ample opportunity to modify and improve the delivery system [5].

In the current research, we prepared a hybrid system of TMZ polymer conjugate and mPEG-PLA. A series of TMZ-polymer conjugates (*mPEG-b-P(CB-{g-COOH; g-TMZ_n})*) were prepared initially and screened, wherein TMZ was conjugated to the polycarbonate block polymer. The obtained conjugates were characterized using NMR and UV spectroscopy. Further, to overcome the drug resistance and blood-brain barrier associated limitations, the hybrid TMZ nanoconjugates were coloaded with sirolimus and surface functionalized with the cell-penetrating peptide (cRGD peptide) and characterized for their *in vitro* and *in vivo* efficacy evaluation in C6-induced syngeneic orthotropic glioma model, wherein brain physiology, survival rate, change in body weight, tumor burden, and hybrid nanoconjugates toxicity were assessed.

Objectives of proposed work

1. Formulation development, optimization, characterization and evaluation of Temozolomide and autophagy modulator co-loaded nano-carriers.
2. Actively targeting of the nanocarriers using a peptide motif for the co-delivery of temozolomide and sirolimus to the brain.
3. *In vitro* evaluation of optimized formulations in glioblastoma cell lines.
4. *In vivo* safety assessment of Temozolomide and autophagy modulator co-loaded nano-carriers.
5. *In vivo* efficacy evaluation of pharmacokinetic and bio-distribution evaluation of the Temozolomide and autophagy modulator co-loaded nano-carriers.

Materials and methods

Materials

Temozolomide (TMZ, >98%), tert-butyl Carbazate, 1H-Benzotriazol-1-yloxytripyrrolidinophosphonium Hexafluorophosphate (PyBOP), N,N-Diisopropylethylamine (DIPEA) were purchased from TCI chemicals (Tokyo, Japan). Dulbecco's Modified Eagle Medium (DMEM), Minimum Essential Medium (MEM), Fetal Bovine Serum (FBS), SnakeSkin™ Dialysis Tubing, 10K MWCO were procured from ThermoFisher Scientific (Massachusetts, United States). Methoxy poly(ethylene glycol) (mPEG, 5000 Da), Annexin V Alexa fluor 488 conjugate, tin(II) 2-ethyl hexanoate, DL-lactide, and propidium iodide (PI) were obtained from Sigma-Aldrich (St. Louis, Missouri, United States). 1,4-Dioxane, and Palladium on carbon (Pd/C) were purchased from spectrochem (Mumbai, India). 3-(4,5-dimethylthiazol-2-yl)-2,5-diphenyl tetrazolium bromide (MTT), N-(3-Dimethylaminopropyl)-N'-ethylcarbodiimide hydrochloride (EDC.HCl), and Hydroxybenzotriazole (HOBt) were obtained from Sisco Research Laboratories (India). All remaining reagents and chemicals used were of analytical grade and bought from local vendors.

Synthesis of polymeric drug conjugate of TMZ (mPEG-b-P(CB-{g-COOH}; g-TMZ_n))

A series of polymeric conjugates of TMZ were synthesized by reacting TMZ hydrazide derivative with amphiphilic mPEG-PCC (*mPEG-b-P(CB-{g-COOH})*) copolymer. As shown in Figure 1, the TMZ-hydrazide derivative was synthesized using a multistep reaction. Initially, TMZ (**1**) was oxidized/converted to TMZ acid (**2**), then reacted with t-butyl

carbazate to form TMZ-BOC-protected hydrazine (**3**), followed by cleavage of BOC using dioxane saturated with HCl into TMZ hydrazide derivative (**4**). An amphiphilic copolymer, mPEG-PCC, with carboxyl pendant groups was synthesized in a multistep reaction, wherein, initially, MBC (**5**) carbonate monomer was synthesized as reported earlier, followed by ring-opening polymerization with mPEG as macroinitiator to yield mPEG-MBC (*mPEG-b-P(CB)*) (**6**) copolymer. The protective benzylic pendant was removed using catalytic hydrogenation to obtain the mPEG-PCC (**7**). TMZ hydrazide derivative (**4**) was reacted to mPEG-PCC (**7**) polymer using EDC/Hobt coupling to obtain polymer conjugate of TMZ (*mPEG-b-P(CB-{g-COOH; g-TMZ_n})*) (**8**). All reactions were carried out under a dry nitrogen atmosphere using the standard protocol. The synthesized intermediates, monomers, and polymers were thoroughly characterized using ¹H NMR (400MHz) and ¹³C NMR (101MHz) spectroscopy using Bruker AVANCE III 400 MHz NMR spectrometer (Billerica, Massachusetts, United States) at 20 °C either using DMSO-d₆ and CDCl₃ with tetramethylsilane (TMS) as an internal reference. High-resolution mass (HRMS) spectra were recorded using an Agilent Technologies 6545 Q-TOF LC/MS system (Agilent Technologies, Inc., California, United States) with electrospray ionization mode to detect the mass of monomers and their adducts.

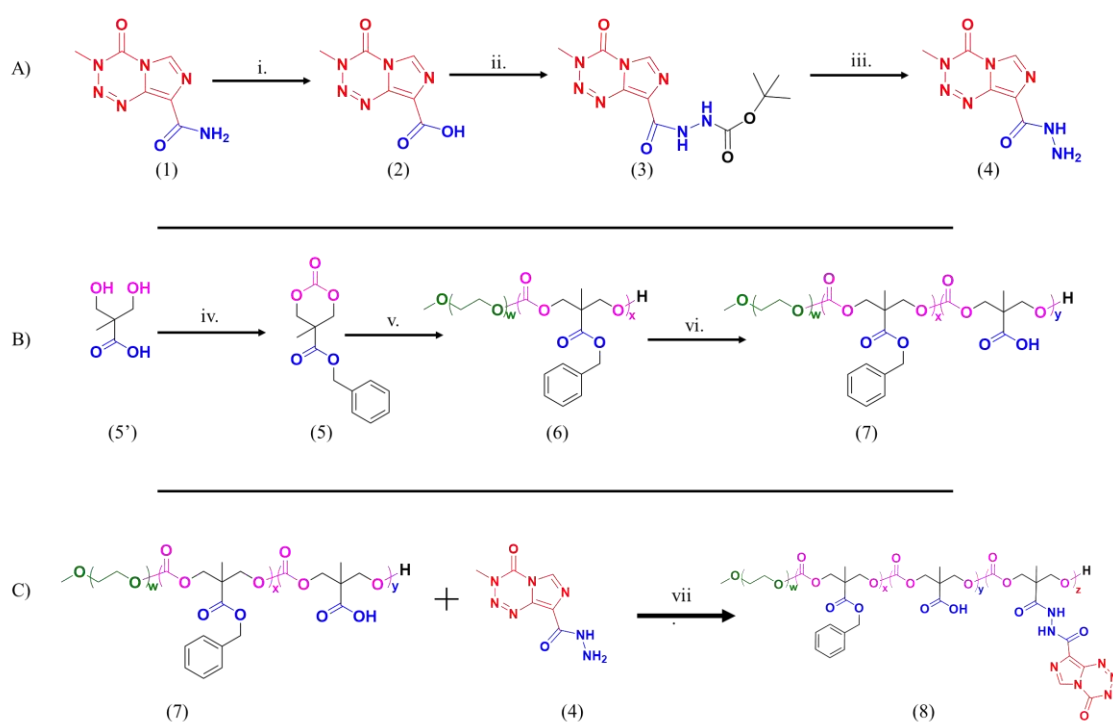


Figure 1. Reaction scheme for the synthesis of temozolomide polymer conjugates. A) Synthesis of TMZ derivatives. i) (**1**), NaNO₂, H₂SO₄, 4-8 °C, overnight, ii) (**2**), t-butyl carbazate, PyBOP, triethylamine, overnight, iii) (**3**), dioxane.HCl, 4-6 h, B) Synthesis of polycarbonate polymer with free COOH group (mPEG-PCC) iv) (**5'**), benzyl bromide, KOH, 100°C, overnight, then triphosgene, pyridine, acetone-dry ice bath, 4 h, v) (**5**), mPEG (Mn. 5000), tin(II)-ethylhexanoate, microwave-assisted ring-opening polymerization, 130 °C, 1 h, vi) (**6**), Palladium on charcoal, H₂, 5 h, C) Synthesis of TMZ-polymer conjugates (*mPEG-PC-g-(TMZ)*) vii) (**4**), (**7**), EDC/HoBT coupling, DIPEA, N₂, 4-8 °C.

As reported, TMZ (1) with a free amide group was oxidized to a free -COOH group [6]. TMZ-A (2) was prepared by dissolving TMZ (1) (2.577 mmol) in 4 ml conc. H₂SO₄, a sodium nitrite solution (9.4 mmol) was added dropwise with continuous nitrogen flow under ice-chilled conditions to remove the gaseous by-product, and the reaction mixture was allowed to stir overnight at room temperature. Further, the reaction mixture containing TMZ-A (2) was precipitated by adding ice-chilled water for 30 min. The precipitated product was thus filtered and dried under vacuum to yield a carboxylic acid derivative of TMZ.

Synthesis of Temozolomide-BOC protected hydrazine (TMZ-BOC) (3)

Briefly, a mixture of TMZ-A (2) (5.128 mmol, 1 eq.), Benzotriazol-1-yl-oxytripyrrolidinophosphonium hexafluorophosphate (PyBOP) (5.641 mmol, 1.1 eq.) and triethylamine (TEA) (1.07 ml) was added in 30 ml of dried acetonitrile. After that, t-butyl carbazate (5.641 mmol, 1.1 eq) was added to the reaction mixture under ice-cold conditions and stirred at room temperature overnight under a nitrogen atmosphere. The following day, the solvent was evaporated under a vacuum and dissolved in dichloromethane (DCM). The obtained crude DCM layer was washed with a saturated sodium chloride solution twice, and the DCM layer was collected, dried over anhydrous sodium sulfate, and evaporated to obtain a thick light yellow waxy liquid. The mixture was then purified using column chromatography, followed by washing with ice-cold diethyl ether to yield pure TMZ-BOC hydrazine (3)

Synthesis of Temozolomide hydrazide (TMZ-H) (4)

TMZ-BOC (3) containing the protective BOC group is highly susceptible to undergo cleavage under acidic conditions to form free amide end group functionality. TMZ-H (4) was synthesized by deprotecting (3) using 1,4-dioxane saturated with HCl in a 100 ml round bottom flask under cold conditions for 4-6 h. Upon completion of the reaction, the remaining solvent was removed using a vacuum, and the mixture obtained was washed with diethyl ether to yield TMZ-H (4) having free amine (-NH₂) end group of hydrazine attached to imidazotetrazine derivative.

Synthesis of mPEG-MBC polycarbonate polymer (mPEG-b-P(CB)) (6)

As reported previously, MBC (5) monomer was synthesised using a multistep reaction. The mPEG-b-P(CB) (6) copolymer was synthesized using microwave-assisted ring-opening polymerization (ROP) of MBC (5) carbonate monomer with mPEG as macroinitiator using

tin(II) ethyl hexanoate $\text{Sn}(\text{Oct})_2$ as a catalyst at 130°C for 1 h [7]. The crude polymer was purified using precipitation by dissolving in chloroform and precipitating with isopropyl alcohol and diethyl ether twice. The purified copolymer was then dried under a vacuum and characterized using NMR spectroscopy.

Synthesis of mPEG-carboxylic polycarbonate copolymer (mPEG-PCC) mPEG-b-P(CB-{g-COOH}) (7)

mPEG-b-P(CB) (**6**) was subjected to catalytic hydrogenation to remove the protective benzylic group and obtain free carboxyl groups on the polycarbonate backbone. Briefly, mPEG-b-P(CB) (**6**) (2.0 g) was dissolved in dried tetrahydrofuran and methanol in a ratio 1:1 and taken in a glass vial to which 400 mg of palladium on carbon (Pd/C) was added under nitrogen flow. Hydrogenation of copolymer was done in hydrogenation parr apparatus at 40-45 psi pressure for 5 h. The copolymer was centrifuged and filtered using celite 545® as a filter aid to remove the remaining Pd/C, followed by solvent removal and drying under vacuum to yield mPEG-PCC (**7**).

Synthesis of temozolomide polymer-drug conjugate (mPEG-b-P(CB-{g-COOH; g-TMZ_n}) (8)

A series of temozolomide-conjugated amphiphilic copolymers were synthesized using EDC-HOBT coupling chemistry. Briefly, a mixture of mPEG-PCC (**7**) (M_n 21 kDa, 1.285 mmole of COOH, 1 eq), 1-Ethyl-3-(3-dimethylaminopropyl) carbodiimide hydrochloride (EDC.HCl) (1.93 mmol, 1.5 eq), N,N-diisopropylethylamine (DIPEA) (3.21 mmol, 2.5 eq) and hydroxybenzotriazole (HOBT) (1.93 mmol, 1.5 eq) were added to 5 ml of dried dimethylformamide (DMF) under ice-cold conditions. After that, the mixture was activated under a nitrogen atmosphere for 0.5 h, followed by the addition of compound (**4**) (0.7, 1, and 1.3 mol eq). The reaction mixture was allowed to stir overnight under a nitrogen atmosphere. After this, the reaction mixture was dialyzed using a snakeskin dialysis membrane (MWCO. 3.5 KDa) against purified water for 6-8 h, and water was replaced every 1 h. The resulting dialysate was taken from the dialysis bag and freeze-dried to yield the mPEG-b-P(CB-{g-COOH; g-TMZ_n}) (**8**).

Synthesis of mPEG-polylactic acid (mPEG-PLA) copolymer (9)

mPEG-PLA (**9**) was synthesized using the previously described microwave-assisted ring-opening polymerization method as shown in Figure 2A [7]. Briefly, DL-Lactide (**9'**) (0.535

g) was polymerized with mPEG (465 g) as a macroinitiator in the presence of tin(II) ethyl hexanoate as a catalyst at 130°C for 1 h. After that, the crude copolymer was allowed to cool at room temperature, followed by purification by means of dissolving in chloroform and precipitating in isopropyl alcohol and diethyl ether twice. The purified mPEG-PLA polymer was dried under a vacuum and analyzed using ¹H NMR spectroscopy.

Synthesis of cRGD-Mal-PEG-poly(lactic acid) (cRGD-PLA) copolymer (10)

cRGD-PLA (**10**) was synthesized using the above method (Figure 2B). Briefly, DL-Lactide (**9'**) (0.535 g) was polymerized with mal-PEG₅₀₀₀ (465 g) as a macroinitiator in the presence of tin(II) ethyl hexanoate as a catalyst at 130°C for 1 h. After that, the crude copolymer was purified using precipitation in isopropyl alcohol and diethyl ether twice. The purified mal-PEG-PLA polymer was dried under a vacuum. The obtained polymer was taken for coupling between cRGD peptide and mal-PEG-PLA using a maleimide coupling reaction in the presence of DMSO as a solvent. The crude was dialysed using purified water for 8 h against the purified water. The obtained dialysate was freeze-dried and characterized using ¹H NMR spectroscopy.

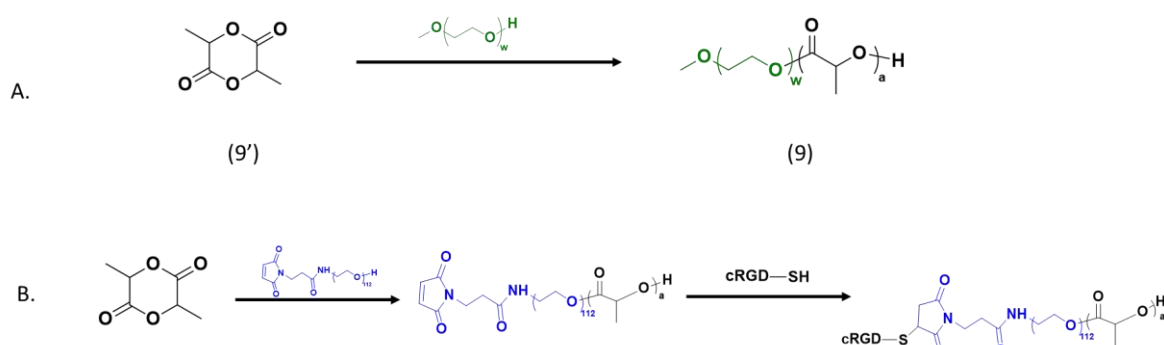


Figure 2. reaction scheme for the synthesis of A) mPEG-PLA, and B) cRGD-PLA

Development of hybrid TMZ nanoconjugate formulation (Hybrid TMZ-NCs)

A hybrid system containing mPEG-b-P(CB-{g-COOH; g-TMZ₄₀} (**8**) and mPEG-PLA (**9**) was developed using the thin film hydration method as reported earlier [8]. Briefly, mPEG-b-P(CB-{g-COOH; g-TMZ₄₀} (75 mg) and mPEG-PLA (25 mg) were dissolved in a DCM and ethanol mixture (3:1) and transferred to a 100 ml round bottom flask, followed by the formation of a thin film by removal of organic solvent using a rotary evaporator. The RBF with a thin film was purged with dried nitrogen gas for 60 min. After that, the thin film was redispersed slowly using a dispersive medium (phosphate-buffered saline) to yield a dispersion mixture. The dispersion was probe sonicated for 20 s at 20 % amplitude under ice-

cold conditions followed by centrifugation at 12000 rpm for 10 min. The obtained supernatant was collected containing hybrid TMZ-NCs and subjected to evaluation for average particle size (PS), polydispersity index (PDI), surface zeta potential (ZP), and surface morphology using scanning electron microscopy (SEM). Further, the hybrid TMZ-NCs were evaluated for UV (for TMZ stability) and colloidal stability. The loading amount to TMZ was calculated using the below-mentioned equation

$$\%TMZ\ loading = \frac{Amount\ of\ TMZ\ present}{Amount\ of\ nanocarrier\ used} \times 100$$

The hydrodynamic diameter and particle size distribution were measured using dynamic light scattering (DLS) (Zetasizer Nano ZS, Malvern Panalytical Ltd, UK) measuring angle 173°. The surface zeta potential (ζ) was determined on Zetasizer Nano ZS (Malvern Panalytical Ltd, United Kingdom). The surface morphology was evaluated by prior surface coating of hybrid TMZ-NCs with gold/chromium target for 120 s using Q150TES sputter coater, Quorum Technologies (Lewes, United Kingdom). After that, the coated particles were evaluated using Field Emission-Scanning Electron Microscopy (FE-SEM) (FEI, Apreo S LoVac, Thermo Fisher Scientific, MA, USA) with a spot size of 9 mm under vacuum.

Development of cRGD targeted hybrid TMZ nanoconjugate formulation coloaded with sirolimus (cRGD targeted hybrid TMZ-NCs)

For the preparation of cRGD targeted hybrid TMZ-NCs, 10% w/w of cRGD-PLA was used encapsulating SIR as whole. Briefly, the SIR was added to the organic component containing polymer, and the remaining method was executed the same as in the above section. The obtained nanoformulation was thoroughly characterized for the particle analysis based on shape, size, uniformity, appearance, loading, and encapsulation efficiency.

Stability studies

The stability studies of the developed hybrid TMZ-NCs were performed under physiological pH at 4 °C and 37 °C. The samples were sealed in a closed vial and incubated to determine the change in particle size and % TMZ remaining in the hybrid TMZ-NCs using dynamic light scattering (DLS) and UV methods, respectively. For the DLS measurements, hybrid TMZ-NCs were taken at concentration of 3 mg/ml and analyzed for the change in particle size and PDI for 7 days. Furthermore, the same samples were used to determine the % drug remaining in the conjugates. For the UV stability analysis, the samples (free TMZ, free

TMZH (**4**), *mPEG-b-P(CB-{g-COOH; g-TMZ₄₀}* (**8**), and Hybrid TMZ-NCs) were taken and analyzed at predetermined time points (0, 6, 12, 24, 48, 72, 96, 120 h) using UV-Vis spectrophotometry. The samples analyzed were withdrawn from the stock and diluted and UV absorbance was evaluated at 328 nm for the % TMZ remaining, and the stability graph or % TMZ remaining was plotted over time.

Cell culture studies

C6 and U87MG glioma cell lines were obtained from the National Centre for Cell Sciences (NCCS, Pune, India). C6 and U87MG cells were maintained in Dulbecco's Modified Eagle Medium (DMEM) and Eagle's Minimum Essential Medium (EMEM) supplemented with 10% fetal bovine serum (FBS) and 1 % penicillin/streptomycin mixture, kept in an incubator at 37 °C with 5% CO₂. The cells were allowed to proliferate until 70-80% confluency was achieved for further experimentation.

Cell viability assay

C6 and U87MG glioma cells were trypsinized, and cells were seeded in a 96-well plate at a cell density of 5000 cells/well and allowed to incubate at 37°C/ 5% CO₂ for 24 h. On the following day, cells were treated with the respective treatment groups (free TMZ, free SIR, and hybrid TMZ-NCs) in a concentration range of TMZ equivalent to 100-1500 µM and 25-1000 µM and sirolimus equivalent to 0.5-50 µM for C6 and U87MG cells, respectively. After 72 h of treatment, media was replaced with fresh media containing 5 mg/ml of 3-(4,5-dimethyl-thiazol-2-yl)-2, 5-diphenyl tetrazolium bromide (MTT) and kept for 4 h in an incubator. After the formation of formazan crystals, the media was discarded, and 200 µL of DMSO was added to each well to dissolve the crystals. The extent of metabolic activity was measured by determining the absorbance at 570 nm and 630 nm using an Epoch microplate spectrophotometer (Biotek Instruments, USA). The % cell viability was calculated by subtracting the absorbance of 630 nm from the 570 nm using the below-mentioned equation [5].

$$\% \text{ Cell Viability} = \frac{\text{Absorbance of sample wells (560 nm)} - \text{absorbance of sample wells (630 nm)}}{\text{Absorbance of control wells (560 nm)} - \text{absorbance of control wells (630 nm)}} \times 100$$

Combination index analysis

The combination index of TMZ and SIR was determined using Compusyn software (version 1.0). From the data observed using cytotoxicity assay TMZ and SIR individually on C6 and U87MG cells, we have used a variable constant and non-constant ratio of TMZ and SIR for analysis. The Chou-Talalay method was used to analyze the combination index of the proposed drug combination. The combination index values obtained were analyzed for synergism (<1) and antagonism (>1) and the combinational ratio was determined.

Apoptosis assay

Apoptosis analysis of developed Hybrid TMZ-NCs was determined using the Annexin-V/PI-kit-based flow cytometry assay. Briefly, C6 and U87MG glioma cells were seeded in a 6-well plate (1×10^5 cells/well). The cells were incubated overnight, followed by the treatment with free TMZ or hybrid TMZ-NCs for 24 h. Thereafter, cells were washed with PBS, trypsinized, centrifuged, resuspended in 1X annexin binding buffer, and stained with annexin-V/propidium iodide in a dark condition for 5 min. Flow cytometry (Beckman Coulter, USA) was used to analyze the apoptosis rate, and data were interpreted using CytExpert V3.0 software [5].

Cell uptake assay

Cellular uptake potential of developed Hybrid TMZ-NCs were determined using qualitative and quantitative method. Briefly, cells (C6 and U87MG) were seeded in a 6-well plate (1×10^5 cells/well) and allowed to adhere for 24 h. Thereafter, the cells were treated with blank C6 dye and C6-loaded hybrid TMZ-NCs and incubated for 4 h. Further, the cells were washed with PBS, fixed with 2% paraformaldehyde for 10 minutes, and counterstained with DAPI for 10 minutes to stain nucleus. For Qualitative analysis, fixed cells were observed under a fluorescence microscope (ZEISS, Germany), and respective microscopic images (DIC, DAPI, C6, and Overlay) were acquired for the treatment groups. Obtained data were interpreted using Zen Blue software V3.4. For Quantitative analysis, the samples were trypsinized, washed with PBS, and evaluated for the quantitative uptake of C6-dye in glioma cells using flow cytometry (Beckman Coulter, USA), and the obtained data were interpreted using CytExpert V3.0 software [5].

C6 cells induced orthotropic glioblastoma implantation in rat brain

C6 glioma cells were incubated in an incubator until 70% of confluency and cells were trypsinized with (0.25% trypsin/EDTA solution), washed with DMEM medium, and suspended in 80 µl of sterile phosphate-buffered saline. Sprague Dawley Male rats, 6-8 weeks old, were used after the approval from the Institutional Animal Ethics Committee (IAEC) of BITS Pilani, with protocol no: IAEC/RES/23/08/Rev-3/32/26, and all the animal experiments were performed as per the Committee for the Purpose of Control and Supervision of Experiments on Animals (CPCSEA) guidelines. For C6 glioma cells implantation, rats were anesthetized with ketamine and xylazine at 90 mg/kg and 9 mg/kg, i.p., respectively. Animals were placed on the stereotaxic apparatus, and the head was shaved, followed by a small incision of 3 cm to expose the skull. A 1 mm burr hole was drilled, and C6 cells (2×10^6) were injected at 2 mm anterior, 3 mm lateral, and 4 mm depth to the bregma at a flow rate of 3 µl/min using Hamilton's syringe. After injection, the needle was kept in the same position additionally for 2 min to avoid backflow. After that, the burr hole was sealed using biodegradable wax, and an incision was sealed using a suture. Animals were placed back in their home cages and observed until they regained consciousness. Animals were continuously observed daily for their change in neurological behaviour, body weight, and right eye bulging, as an indicator of tumor development.

In vivo efficacy studies of cRGD targeted hybrid TMZ NCs in C6 cells induced orthotropic rat glioma model

Briefly, C6 glioma cells bearing rats were randomly taken and kept for 9 days, followed by the start of the treatment phase from day 10th with treatment groups (n=5) including positive control, free TMZ, free SIR, Hybrid TMZ NCs, non-targeted Hybrid TMZ NCs (SIR-loaded), and cRGD targeted hybrid TMZ NCs (SIR-loaded). All drug treatments were given at the dose equivalent to 10 mg/kg of TMZ and 1 mg/kg of SIR thrice a week for next 30 days. The animals were regularly monitored for their change in body weight, locomotion, and neurobehavioral activity. On day 40th, animals were sacrificed per the protocol, and the blood and major organs (such as heart, lungs, liver, spleen, kidney, etc.) were excised for the histopathological toxicity evaluation. In addition, the excised brains of all the animals were isolated and evaluated for physical appearance, brain weight, hemispherical width ratio (RH/LH), and histopathological evaluation.

Statistical analysis

Results are expressed as mean \pm SD or mean \pm SEM. All the obtained data were analysed using ANOVA (analysis of variance) followed by Tukey's test for comparison between treatment groups. $p < 0.05$ was considered as statistically significant.

Results

Characterisation of Temozolomide conjugated amphiphilic copolymer (mPEG-b-P(CB-{g-COOH; g-TMZ_n}) (8)

A series of temozolomide-conjugated amphiphilic copolymers (mPEG-b-P(CB-{g-COOH; g-TMZ})) was synthesized in a multistage reaction, as shown in the synthesis scheme (figure 1). In phase A, the hydrazine derivative of TMZ (4) was synthesized from TMZ. Starting from synthesizing 8-carboxylic acid derivatives of temozolomide (TMZ-A) (2). The oxidation reaction of the free NH₂ group to the free -COOH group was followed by precipitation using ice-chilled water to yield white precipitate (91% yield) and characterized using NMR spectroscopy. Figure 3A showed compound 2 (¹H NMR 400 MHz, DMSO) peaks corresponding to δ 8.79 (s, 1H), 3.87 (s, 3H), wherein the disappearance of two protons of NH₂ of TMZ at δ 7.68-7.81 confirms the conversion of free NH₂ to COOH group. Figure 4B shows ¹³C NMR (101 MHz, DMSO) shows peaks at δ 161.86, 139.11, 136.50, 129.11, 127.81, 36.36 Mass spectroscopy ESI-TOF data showing [M+Na]⁺ at 218.0271 m/z and [M+1]⁺ ion peak at 196.0464 (mol. formula C₆H₅N₅O₃; cal. [M+1]⁺=196.0426) (Figure 3B). Furthermore, the HPLC elution (Figure 5B) of compound 2 shifted to (3.44 \pm 0.002) min from (4.24 \pm 0.005) for compound 1, confirming the synthesis of an 8-carboxylic derivative of TMZ (2)

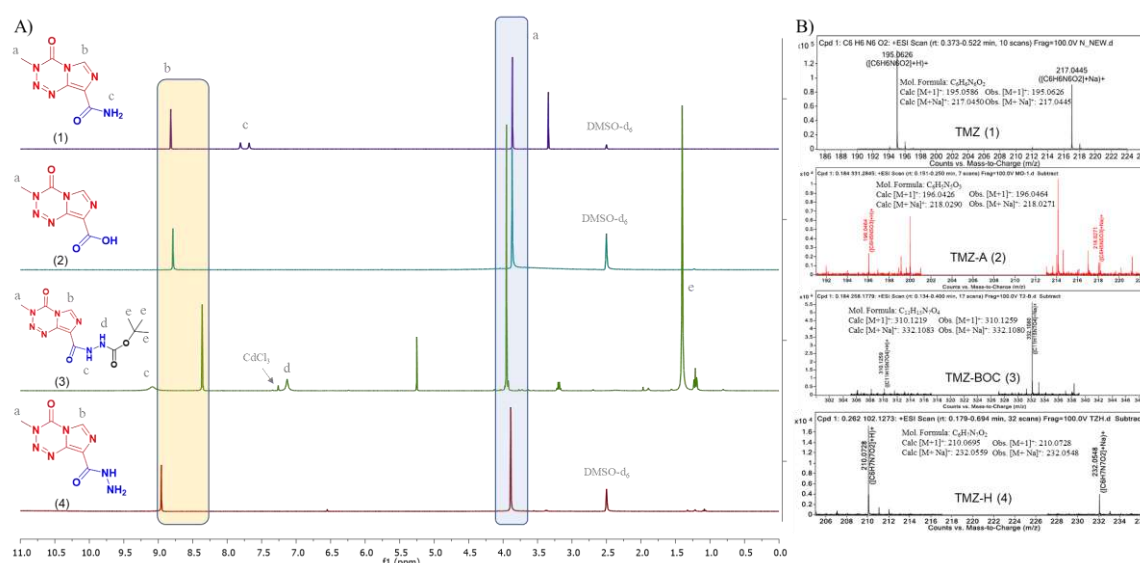


Figure 3. Characterization of TMZ and its derivatives. A) ¹H NMR and B) ESI-TOF HR-Mass spectrometry of TMZ (1), TMZ-A (2), TMZ-BOC (3), and TMZ-H (4).

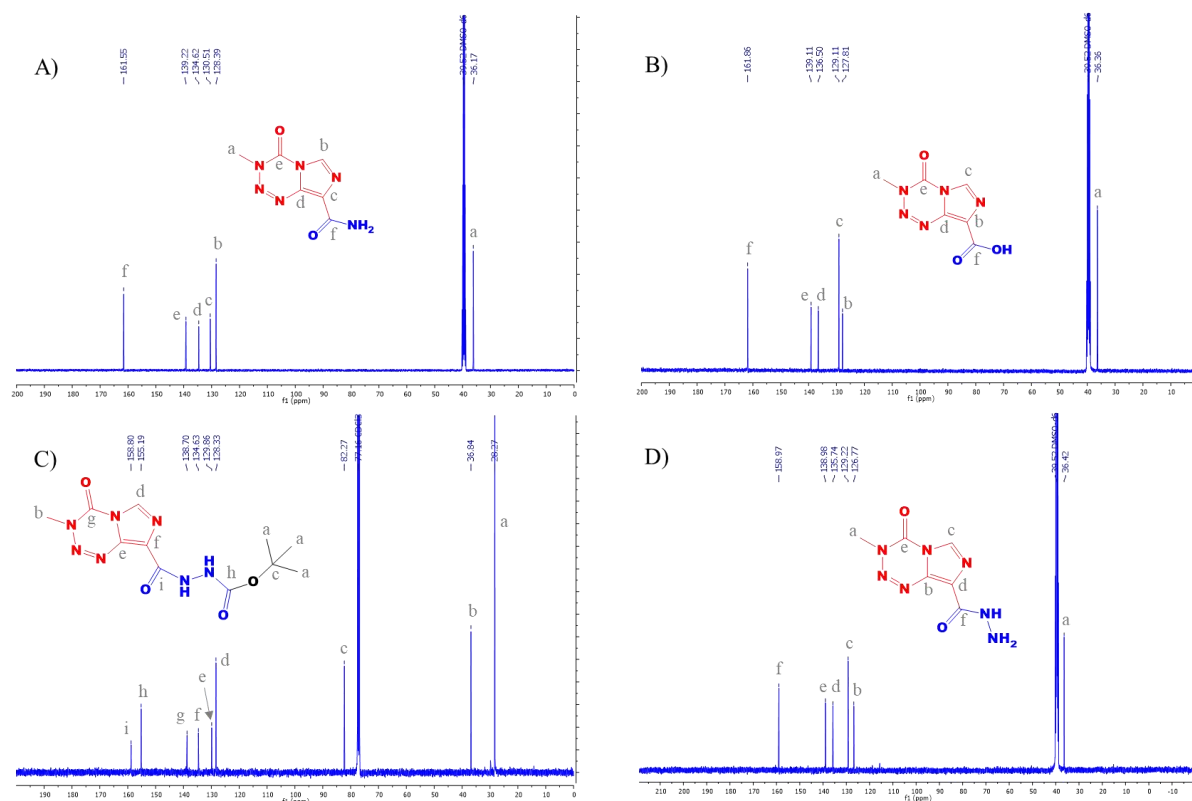


Figure 4. ^{13}C NMR spectrum of A) TMZ (1), B) TMZ-A (2), C) TMZ-BOC (3), and D) TMZ-H (4) using DMSO- d_6 and CdCl_3 as a solvent

After that, free $-\text{COOH}$ of compound **2** was protected with t-butyl carbazate to yield BOC-protected temozolomide hydrazine (TMZ-BOC) (**3**) using PyBOP coupling chemistry. The crude obtained was purified using flash chromatography to yield a pure light-yellow solid with a 62.1% yield. Figure 3A showed ^1H NMR (400 MHz, CDCl_3) peak at δ 9.08 (s, 1H), 8.36 (s, 1H), 7.13 (s, 1H), 3.95 (s, 3H), 1.40 (s, 9H), with the presence of 9 protons at δ 1.40 shows attachment of BOC group to the compound **2**. Figure 4C showed ^{13}C NMR (101 MHz, CDCl_3) δ 158.67, 155.06, 138.57, 134.50, 129.73, 128.20, 82.14, 36.71, 28.14. Mass spectroscopy data shows $[\text{M}+\text{Na}]^+$ at 332.1080 m/z and $[\text{M}+1]^+$ ion peak at 310.1259 (mol formula $\text{C}_{11}\text{H}_{15}\text{N}_7\text{O}_4$; cal. $[\text{M}+1]^+=310.1219$) (Figure 3B). The HPLC elution of compound **3** shifted to (25.58 ± 0.02) min from (3.44 ± 0.002) for compound **2** (Figure 5B), confirming the attachment of BOC group to yield TMZ-BOC (**3**). Subsequently, the deprotection of the BOC group was done using dioxane saturated with HCl, followed by washing with diethyl ether to obtain white powder (65% yield). Figure 3A showed ^1H NMR (400 MHz, DMSO) δ 8.95 (s, 1H), 3.89 (s, 3H), with the disappearance of 9 protons peak from compound **3** to yield compound **4**. Figure 4D showed ^{13}C NMR (101 MHz, DMSO) δ 158.97, 138.98, 135.74, 129.22, 126.77, 36.42. Mass spectroscopy ESI-TOF data reveals $[\text{M}+\text{Na}]^+$ at 232.0548 m/z and $[\text{M}+1]^+$ at 210.0728 (mol formula $\text{C}_6\text{H}_7\text{N}_7\text{O}_2$; cal. $[\text{M}+1]^+=210.0695$) (Figure 3B). HPLC elution of compound **4** shifted to (3.66 ± 0.005) min from (25.58 ± 0.02) for compound **3** (Figure 5B), which is supported by UV spectroscopy data showing its absorption maxima at

328 nm (Figure 5A), signifying the integrity of temozolomide after the synthesis of its hydrazine derivative (**4**).

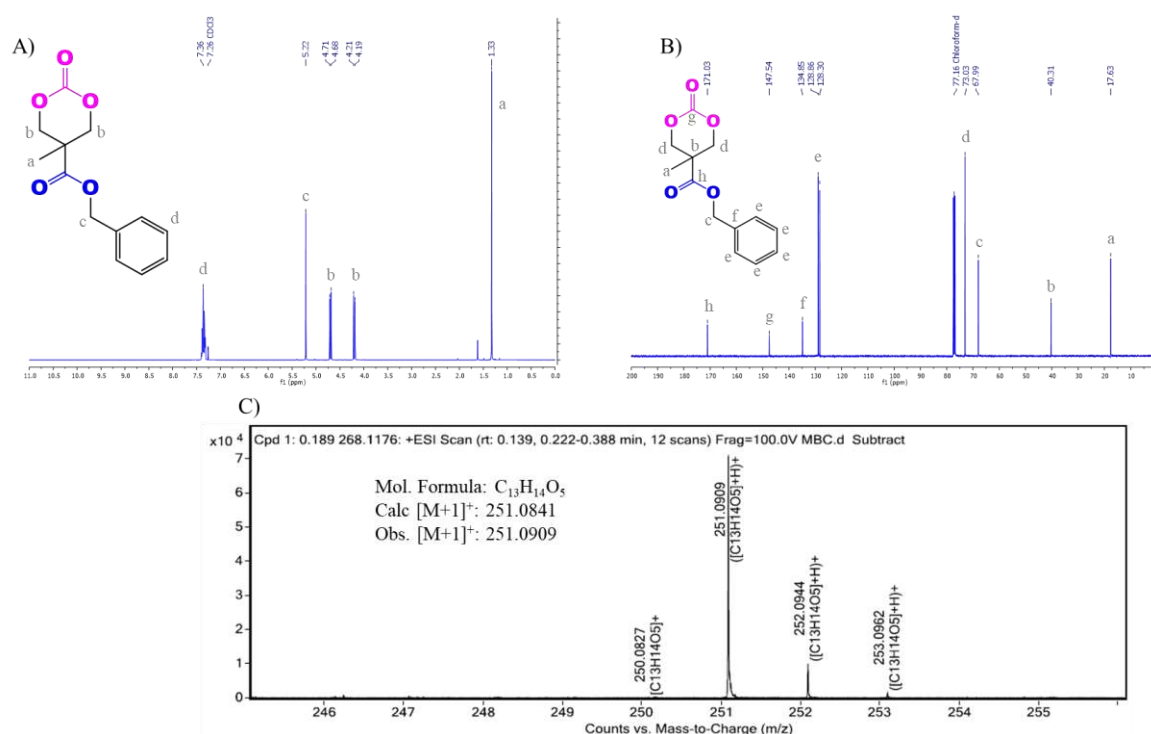


Figure 6. Characterization of MBC cyclic carbonate monomer using A) ^1H NMR, B) ^{13}C NMR, and C) ESI-TOF HR-mass spectrometry

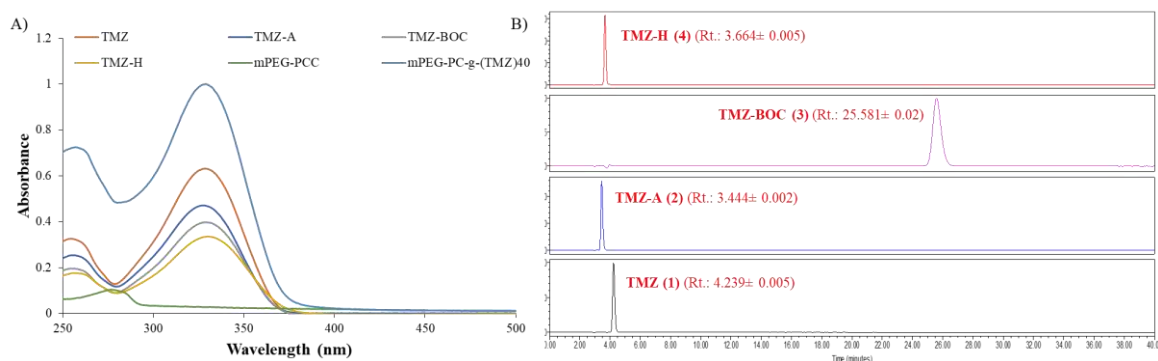


Figure 5. Characterisation of TMZ and its derivatives using A) UV-Vis spectra, and B) HPLC chromatogram

In the phase B, cyclic monomer 5-methyl-5-benzyloxycarbonyl-1, 3-dioxane-2-one (MBC) was synthesized in a two-step reaction as reported earlier [9]. The purified product was characterized using NMR and Mass spectroscopy. Figure 6 shows ^1H NMR (400 MHz, CDCl_3) δ 7.36 (s, 5H), 5.22 (s, 2H), 4.70 (d, $J = 10.9$ Hz, 2H), 4.20 (d, $J = 10.9$ Hz, 2H), 1.33 (s, 3H) and ^{13}C NMR (101 MHz, CDCl_3) δ 171.03, 147.54, 134.85, 128.86, 128.30, 73.03, 67.99, 40.31, 17.63, with $[\text{M}+1]^+$ ion peak at m/z 251.0909 da (mol. formula= $\text{C}_{13}\text{H}_{14}\text{O}_5$; cal. Mass= 250.0841 da), indicating successful synthesis of compound **5**. Microwave-assisted

ring-opening polymerization of MBC (**5**) was initiated in the presence of mPEG as macroinitiator and Sn(Oct)₂ as a catalyst to obtain methoxy-terminated PEGylated copolymer (mPEG-b-P(CB)) (**6**) with a yield of 70%. Figure 7 shows ¹H NMR (400 MHz, CDCl₃) characteristic peak at δ 7.37 – 7.26 (C₆H₅), δ 5.18 – 5.07 (CH₂-Bn), δ 4.35 – 4.19 (CH₂-O), δ 3.64 (CH₂ of PEG), δ 3.38 (CH₃-PEG), δ 1.28 – 1.16 (CH₃) and ¹³C NMR (101 MHz, CDCl₃) δ 172.00, 154.44, 135.47, 128.68, 128.49, 128.44, 128.09, 70.68, 68.70, 67.16, 46.66, 17.51. Then, protective bulky benzylic groups of compound **6** were removed using catalytic hydrogenation in the presence of Pd/C to obtain mPEG-PCC (**7**) with the free carboxylic pendant group on the polymer backbone (60% yield). Figure 8 shows ¹H NMR (400 MHz, DMSO) peak at δ 13.6-12.8 (COOH) 4.22 – 4.11 (CH₂), δ 3.49 (CH₂-PEG), δ 3.21 (CH₃), δ 1.11 (CH₃) and reduction in the number of bulky benzylic protons at δ 7.32 (C₆H₅), δ 5.10 (CH₂), and ¹³C NMR (101 MHz, DMSO) δ 176.62, 175.07, 173.51, 154.20, 153.97, 151.47, 139.18, 128.43, 128.04, 127.55, 124.92, 71.30, 69.81, 68.88, 67.03, 63.86, 63.58, 49.48, 47.48, 45.67, 34.39, 30.44, 25.14, 21.04, 16.94, indicates the reduction in protective benzylic units of the polycarbonate block copolymer to give free carboxylic pendent groups in compound **7**.

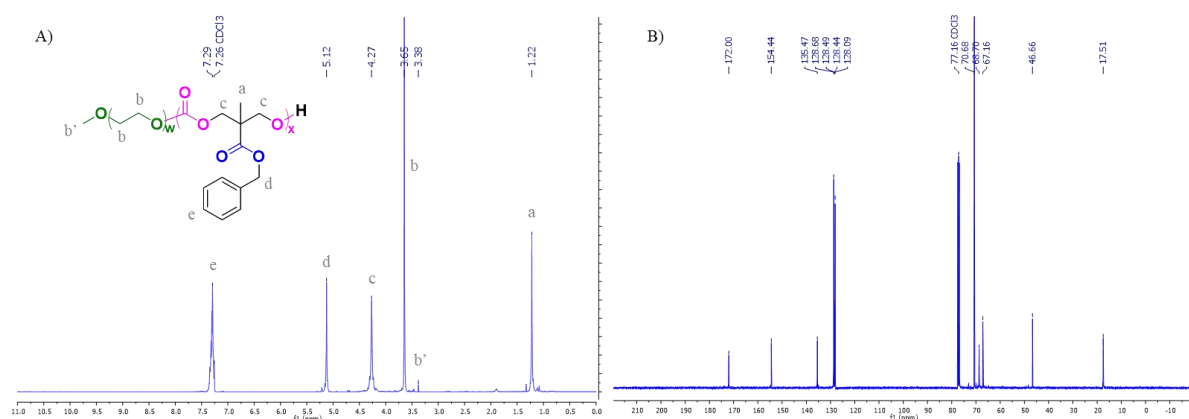


Figure 7. Characterization of mPEG-b-P(CB) carbonate polymer using A) ¹H NMR and B) ¹³C NMR spectroscopy

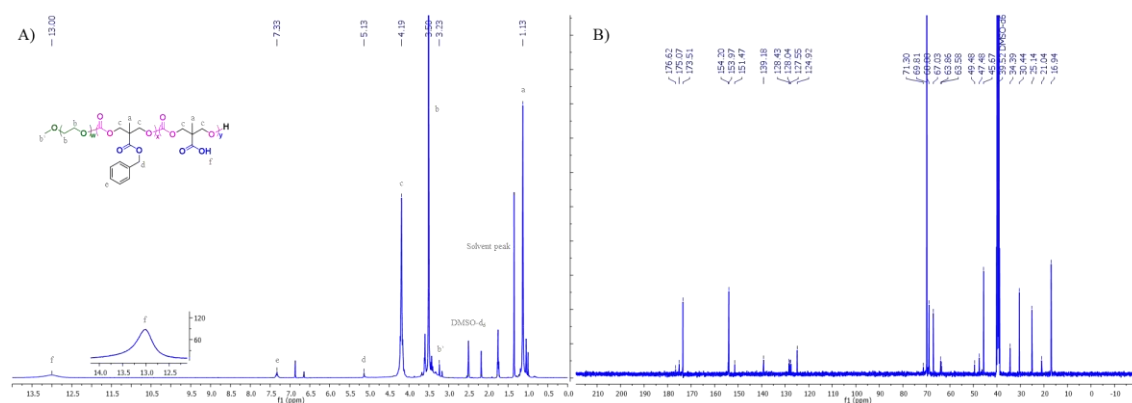


Figure 8. Characterization of mPEG-MCC carbonate polymer using A) ¹H NMR and B) ¹³C NMR spectroscopy

Lastly, Carbodiimide/N-hydroxybenzotriazole (HOBt) coupling chemistry was utilized for grafting the hydrazine derivative of TMZ (4) to the free carboxylic pendent of the polycarbonate polymer backbone of compound 7 to yield the series of temozolamide conjugated amphiphilic copolymer (mPEG-b-P(CB-{g-COOH; g-TMZ_n}) (8). Figure 9 shows ¹H NMR (400 MHz, DMSO) δ 10.31(-NH-NH-), 10.05 (-NH-NH-), 8.84 (N-CH=N- of TMZ), 7.32 (C₆H₅ of MBC), 5.13 (CH₂-Bn), 4.19 (CH₂-), 3.87 (N-CH₃ of TMZ), 3.51 (CH₂-PEG), 3.16 (CH₃-PEG), 2.50 (DMSO-d₆), 1.11 (CH₃-Polymer), indicating the synthesis of mPEG-b-P(CB-{g-COOH; g-TMZ₄₀}), and ¹³C NMR (101 MHz, DMSO) δ 197.08, 173.81, 173.75, 173.70, 158.80, 154.12, 147.56, 139.13, 135.13, 128.76, 88.25, 74.13, 73.94, 69.80, 69.06, 45.70, 45.29, 36.23, 17.16, 15.66. The above-synthesized copolymers were characterized based on TMZ units attached equivalent to 20, 40, and 60 units grafted to the polymer backbone (7), and their average molecular weight number is represented in Table 1.

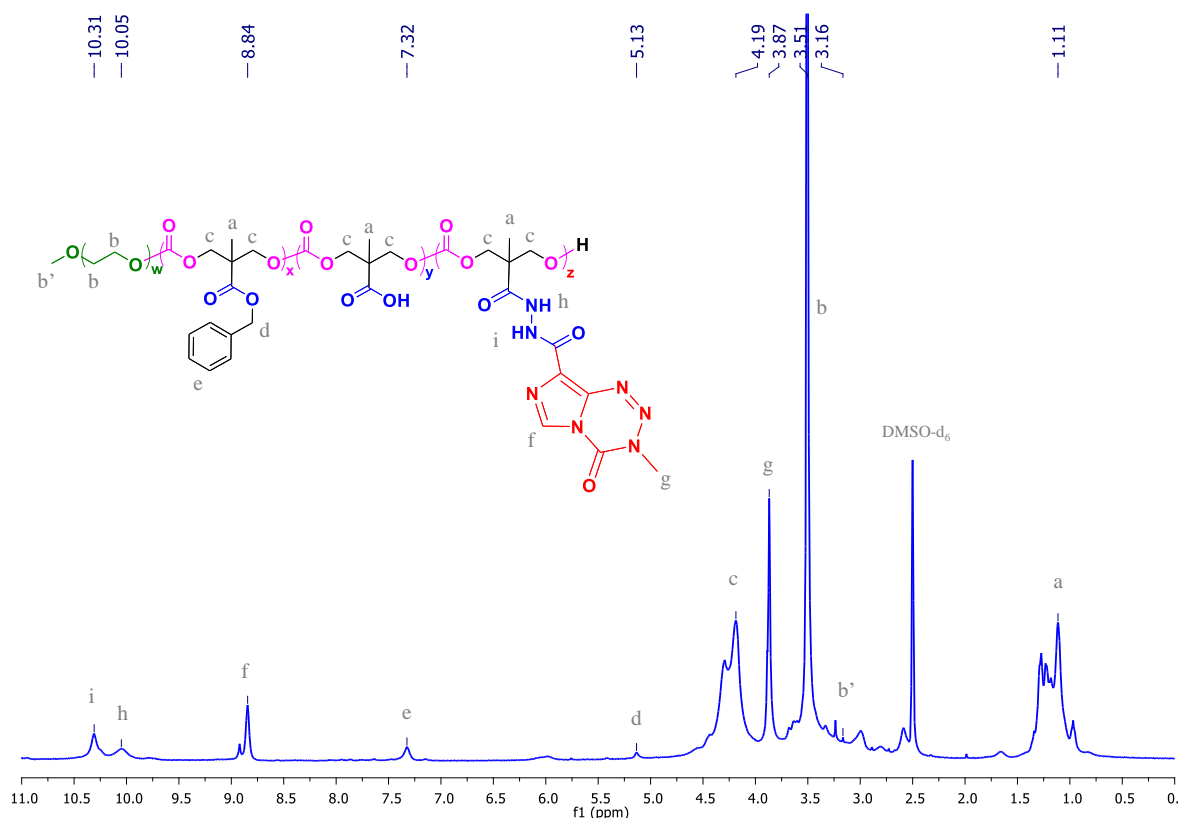


Figure 9. ¹H NMR spectra of mPEG-b-P(CB-{g-COOH; g-TMZ})

Characterization of mPEG-terminated lactide copolymer (mPEG-PLA) (9)

Compound 9 was synthesized using ring-opening polymerization of the D-L lactide in the presence of mPEG as a macroinitiator using tin(II) ethyl hexanoate as a catalyst. Figure 10 shows ¹H NMR (400 MHz, CDCl₃) peak at δ 5.15 (O-CH-C=O), 3.63 (CH₂-PEG), 3.37

(CH₃-PEG), 1.55 (CH-CH₃) with an average molecular weight of 10 KDa and ~70 units of lactic acid, and ¹³C NMR (101 MHz, CDCl₃) δ 169.49, 77.16, 70.68, 69.12, 59.16, 16.87, 16.77.

Table 1. Loading efficiencies of nanoconjugates

Formulation	Loading efficiency (% w/w)
TMZ	n.a.
TMZH	n.a.
mPEG-b-P(CB-{g-COOH; g-TMZ ₂₀ })	16.8%
mPEG-b-P(CB-{g-COOH; g-TMZ ₄₀ })	28.7%
mPEG-b-P(CB-{g-COOH; g-TMZ ₆₀ })	37.99%
Hybrid TMZ NCs*	21.56%

*mPEG-b-P(CB-{g-COOH; g-TMZ₄₀})

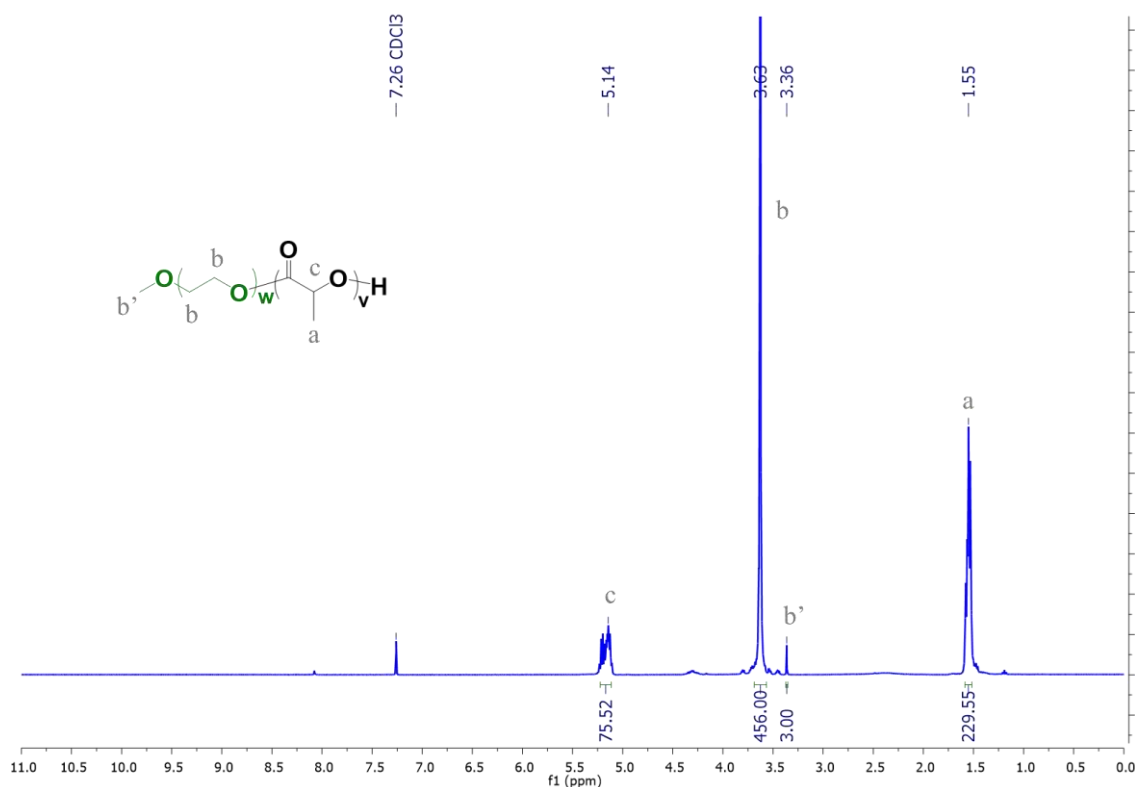


Figure 10. ¹H NMR spectra of mPEG-PLA

Characterization of cRGD-Mal-PEG-poly(lactic acid) (cRGD-PLA) copolymer (10)

Compound **10** was synthesised in a multistep reaction, wherein, mal-PEG-PLA was synthesised using ROP of Mal-PEG₅₀₀₀ and D-L lactide. Figure 7 A&B shows shows ¹H

NMR (400 MHz, CDCl₃) peak at δ 6.67 (maleimide), 5.14, 5.13, (O-CH-C=O), 3.63, (CH₂-PEG), 1.55 (CH-CH₃) with an average molecular weight of 8.5 KDa and ~50 units of lactic acid, and ¹³C NMR (101 MHz, CDCl₃) δ 169.71, 169.45, 70.66, 69.52, 69.27, 69.10, 68.90, 16.85, 16.75. Further, the maleimide-thiol coupling was utilized to obtain cRGD-PLA. Figure 7 C&D shows ¹H NMR (400 MHz, CDCl₃) peak at δ 7-8.5 (cRGD peptide protons), 5.19 (O-CH-C=O), 3.50 (CH₂-PEG), 1.46 (CH-CH₃) with an average molecular weight of 8 KDa and ~45 units of lactic acid, and ¹³C NMR (101 MHz, CDCl₃) δ 169.21, 169.07, 69.79, 68.90, 68.68, 39.52, 20.35, 16.47, 16.94, 77.16, 70.68, 69.12, 59.16, 16.87, 16.77. The disappearance of maleimide protons in Figure 7 C and the appearance of cRGD peptide protons at δ 7-8.5 indicates the successful coupling of cRGD.

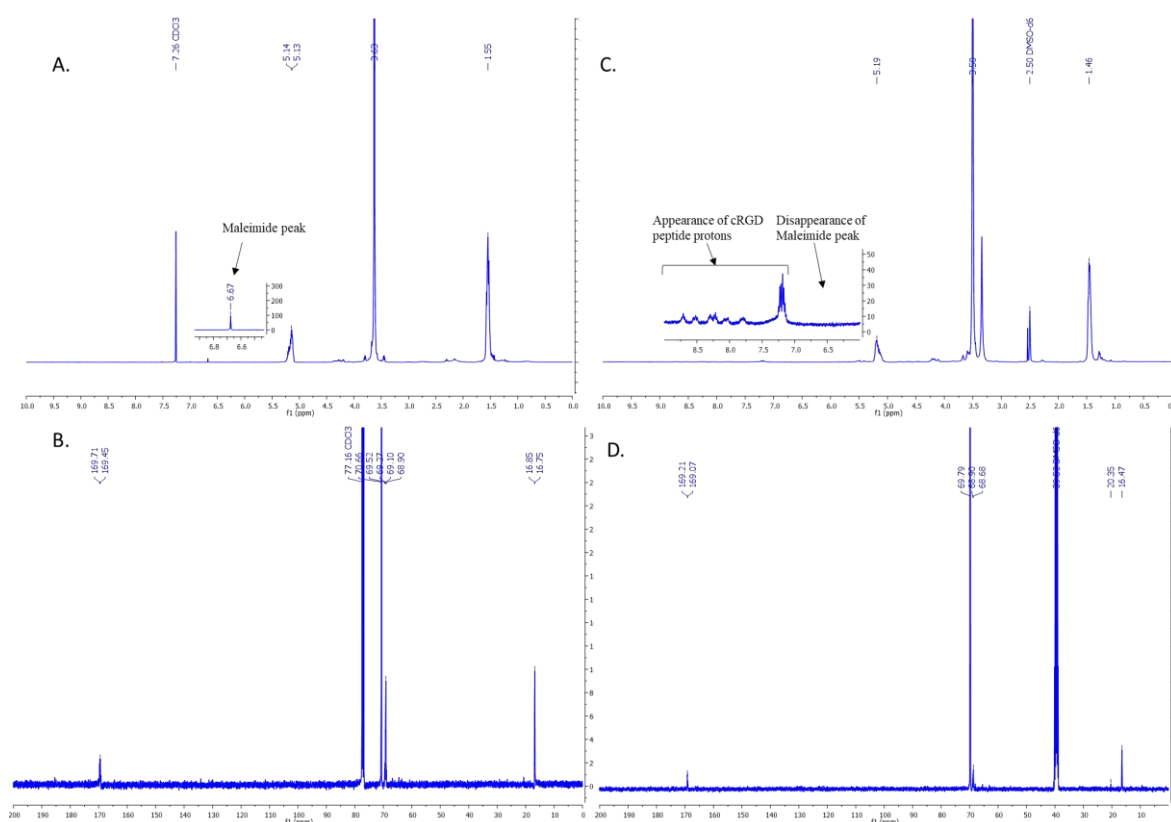


Figure 11. ¹H and ¹³C NMR spectrum of A & B) Mal-PEG-PLA and C & D) cRGD-PLA

mPEG-b-P(CB-{g-COOH; g-TMZ} (8) NCs characterization

A series of conjugates were synthesized with varying TMZ units, i.e., ~20, 40, and 60. The obtained mPEG-b-P(CB-{g-COOH; g-TMZ₂₀}, mPEG-b-P(CB-{g-COOH; g-TMZ₄₀}, and mPEG-b-P(CB-{g-COOH; g-TMZ₆₀} were initially screened based on the particle size and surface morphology under varying pH conditions, including pH 5.0, 6.0, and 7.4, using DLS

and SEM, respectively (Figure 12). mPEG-b-P(CB-{g-COOH; g-TMZ₂₀}) assembled in an aqueous medium with a particle size of >200 nm range, with comparatively low loading efficiency (Figure 12 and Table 1). Although mPEG-b-P(CB-{g-COOH; g-TMZ₆₀}) demonstrated significantly higher loading capacity, it assembled into the aqueous dispersive medium with a larger particle size of >500 nm, i.e., unsuitable for the *in vitro* and *in vivo* experimentation. Interestingly, mPEG-b-P(CB-{g-COOH; g-TMZ₄₀}) depicted an average size of 90.9 ± 3.80 nm in physiological conditions with a surface zeta potential of -12.06 ± 0.86 mV, which could be used as a potential nanoconjugate with optimal size and improved loading capacity.

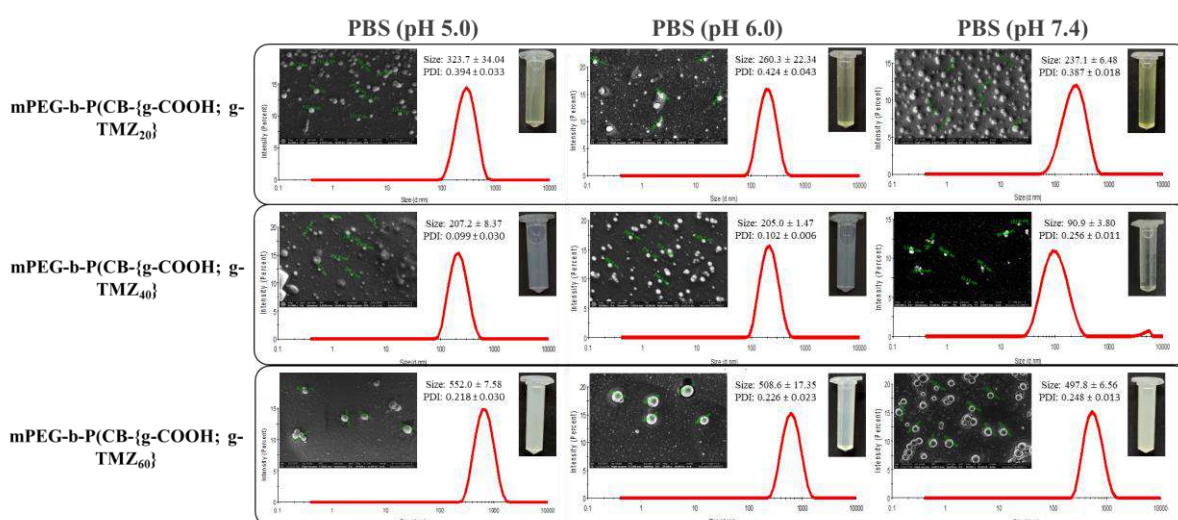


Figure 12. Physiochemical characterization of TMZ-polymer conjugates (mPEG-b-P(CB-{g-COOH; g-TMZ₂₀}) mPEG-b-P(CB-{g-COOH; g-TMZ₄₀}) mPEG-b-P(CB-{g-COOH; g-TMZ₆₀}) in various dispersive mediums (PBS; 10 mM pH 5.0, PBS; 10 mM pH 6.0, and PBS; 10 mM pH 7.4) using Dynamic light scattering (DLS), Scanning electron microscopy (SEM) images, and their representative pictographs

Characterization of cRGD targeted hybrid nanoconjugates composed of component 8, 9, and 10 (cRGD targeted hybrid TMZ-NCs)

The colloidal and TMZ stability after conjugation to the polymeric backbone is still the bottleneck and must be addressed. Therefore, the mPEG-b-P(CB-{g-COOH; g-TMZ₄₀}) (**8**), compound **9** or **10** were used in a 3:1 ratio to overcome the associated stability limitations. The cRGD targeted hybrid TMZ-NCs was prepared using the thin film hydration method. The resulting cRGD targeted hybrid TMZ-NCs depicted an average particle size of 155.0 ± 0.51 nm with a narrow polydispersity index of 0.124 ± 0.014 and a surface zeta potential of ζ : -3.8 ± 0.118 mV while hybrid TMZ NCs exhibited size of 105.7 ± 0.99 nm with polydispersity index of 0.106 ± 0.033 and a surface zeta potential of ζ : -6.79 ± 1.61 mV (Figure 13 A, B, C, F & G). The SEM images confirmed the particles obtained were uniform

in size and spherical in morphology. Simultaneously, the loading capacity of the hybrid nanoconjugate was significantly higher, equivalent to ~21.56% w/w, proving the improved drug loading capacity in the final formulation (Table 1).

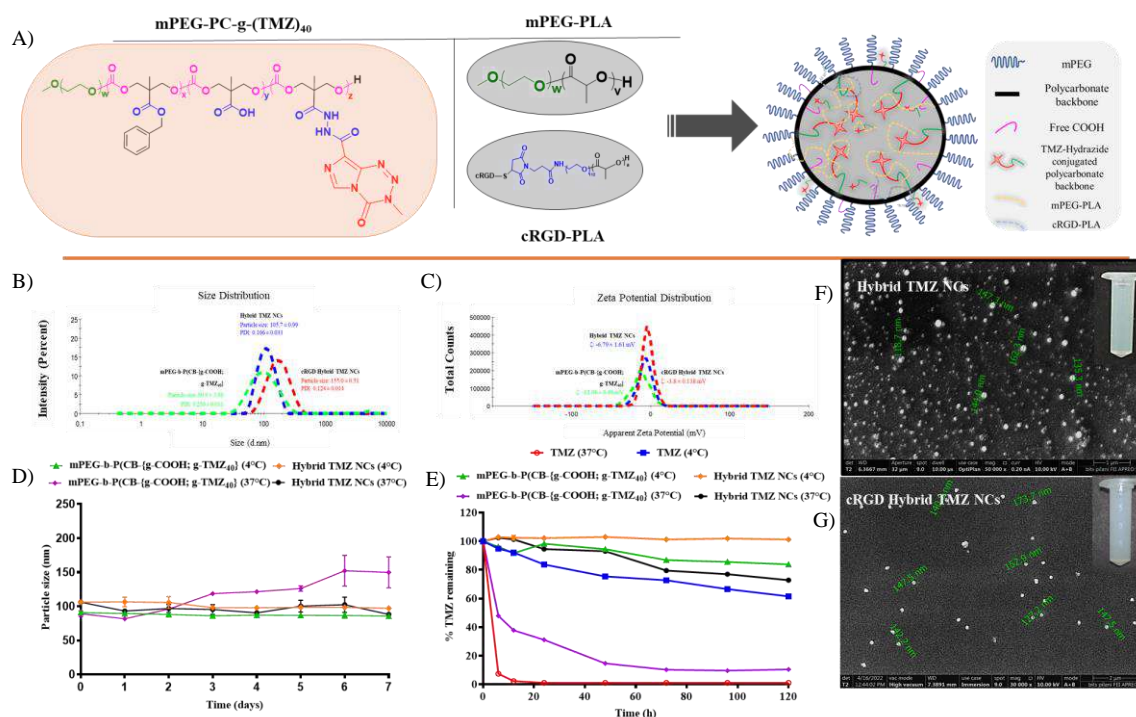


Figure 13. Representation and characterization of cRGD targeted and non-targeted hybrid nanoconjugates. A) Schematic representation of hybrid nanoconjugates in combination with mPEG-b-P(CB-{g-COOH; g-TMZ₄₀}) and mPEG-PLA/cRGD-PLA. Physicochemical analysis based on B) average particle size, C) surface zeta potential, F) surface morphology using scanning electron microscopy (SEM), D) DLS-based colloidal stability, and E) UV-based TMZ stability evaluation of nanoconjugates.

Hybrid TMZ nanoconjugate: UV and size stability

The colloidal stability of the nanoconjugates was determined in physiological pH at 4° and 37° C for up to 7 days. The mPEG-b-P(CB-{g-COOH; g-TMZ₄₀}) demonstrated a marked change in particle size after 2 days, while Hybrid TMZ-NCs was colloidally stable even at 37°C for over 7 days. At 4°C, mPEG-b-P(CB-{g-COOH; g-TMZ₄₀}) and Hybrid TMZ-NCs showed no significant change in particle size over the complete study.

TMZ exhibits hydrolytic degradation to form MTIC and AIC under physiological pH with a half-life of 1.8-1.9 h. The nanoconjugate decomposition rate was determined using UV-Vis spectrophotometry at characteristic TMZ wavelength (328-330 nm) for 120 h. However, the conjugation of TMZ (mPEG-b-P(CB-{g-COOH; g-TMZ₄₀}) has improved the stability up to 5.88 h, but it is still not significantly stable for the in-vivo treatment phase. Upon formulation of mPEG-b-P(CB-{g-COOH; g-TMZ₄₀}) with mPEG-PLA (9), the stability half-life of Hybrid TMZ-NCs was improved considerably to over 120 h with $t_{1/2}$ of ~194 h. Therefore,

the hybrid nanoconjugate improved stability by >100 folds compared to the free drug (Figure 13 D&E).

In-vitro cell toxicity and uptake assay of hybrid nanoconjugates

The cellular viability profiles of treatment groups (including free TMZ and Hybrid TMZ-NCs) were determined in C6 and U87MG glioma cell lines, as shown in Fig 13 A&B. The Hybrid TMZ-NCs significantly improved IC₅₀ to ~645 μ M compared to ~1125 μ M for free TMZ in C6 glioma cells. Similarly, in U87MG cells, the Hybrid TMZ-NCs showed an IC₅₀ of ~866 μ M compared to ~738 μ M for free TMZ, indicating the inherent pharmacological activity of TMZ after conjugation and its hybrid dispersion with mPEG-PLA (9).

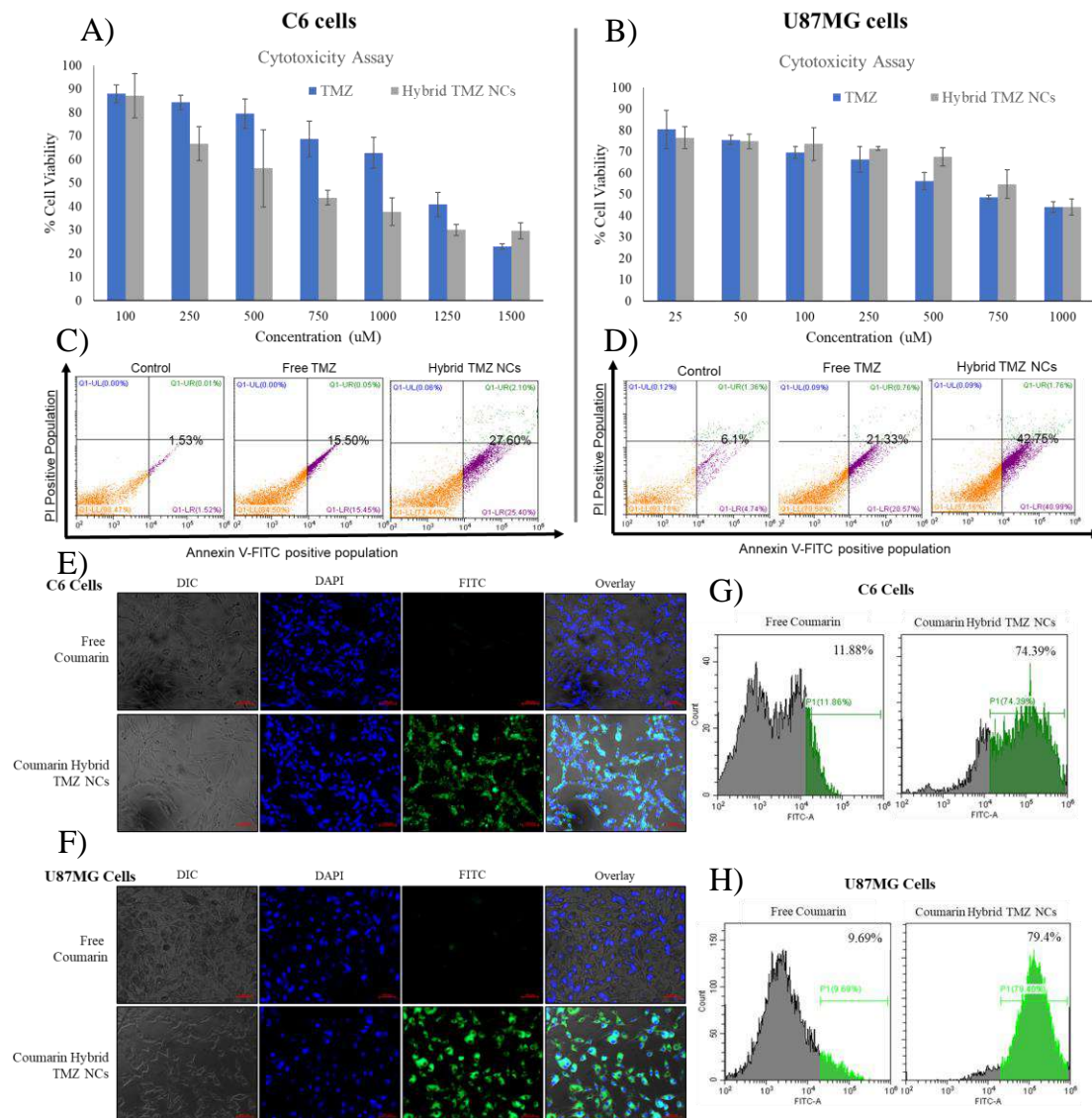


Figure 14. In-vitro cell-based evaluation of hybrid nanoconjugates in glioma cells. Cell cytotoxicity using MTT assay in A) C6 and B) U87MG glioma cells. Annexin-V/PI-based apoptosis assay in C) C6 and D) U87MG glioma cells. Coumarin (C6)-based cellular uptake assay. E) & F) Qualitative evaluation using microscopy in C6 and U87MG glioma cells, G) & H) Quantitative uptake estimation using flow cytometry in C6 and U87MG glioma cells, respectively

The cellular uptake of hybrid TMZ nanoconjugate was analyzed in C6 and U87MG glioma cells using coumarin-6 as a fluorescent probe, and cells were counterstained with DAPI (blue). (Figure 13 E&F), indicating an improved uptake in the glioma cells. The same was confirmed using flow cytometry analysis. The developed Hybrid TMZ-NCs exhibited significantly improved uptake efficiency in both C6 and U87MG glioma cells with ~74% and ~79% uptake efficiency, respectively ($p < 0.001$) (Figure 13 G&H). Thus, it signifies the application of hybrid polymers for improved delivery to glioma cells.

Apoptosis analysis of hybrid nanoconjugates

Apoptosis analysis was performed using Annexin /PI staining flow-cytometry-based method to determine the apoptosis pattern of the treatment groups (free TMZ and Hybrid TMZ-NCs) in C6 and U87MG glioma cells. Figure 13 C&D represents the apoptosis rate in C6 glioma cells, wherein the Hybrid TMZ-NCs demonstrated significant improvement in total apoptosis of 27.6% (early apoptosis: 25.4% and late apoptosis: 2.1%) compared to free TMZ with apoptosis of 15.5% (early apoptosis: 15.45% and late apoptosis: 0.05%). Similarly, in U87MG cells, the Hybrid TMZ-NCs showed a significantly improved total apoptosis of 42.75% (early apoptosis: 40.99% and late apoptosis: 1.76%), compared to free TMZ with total apoptosis of 21.33% (early apoptosis: 20.57% and late apoptosis: 0.76%), indicating the inherent pharmacological responses of the TMZ molecule.

Combination index analysis

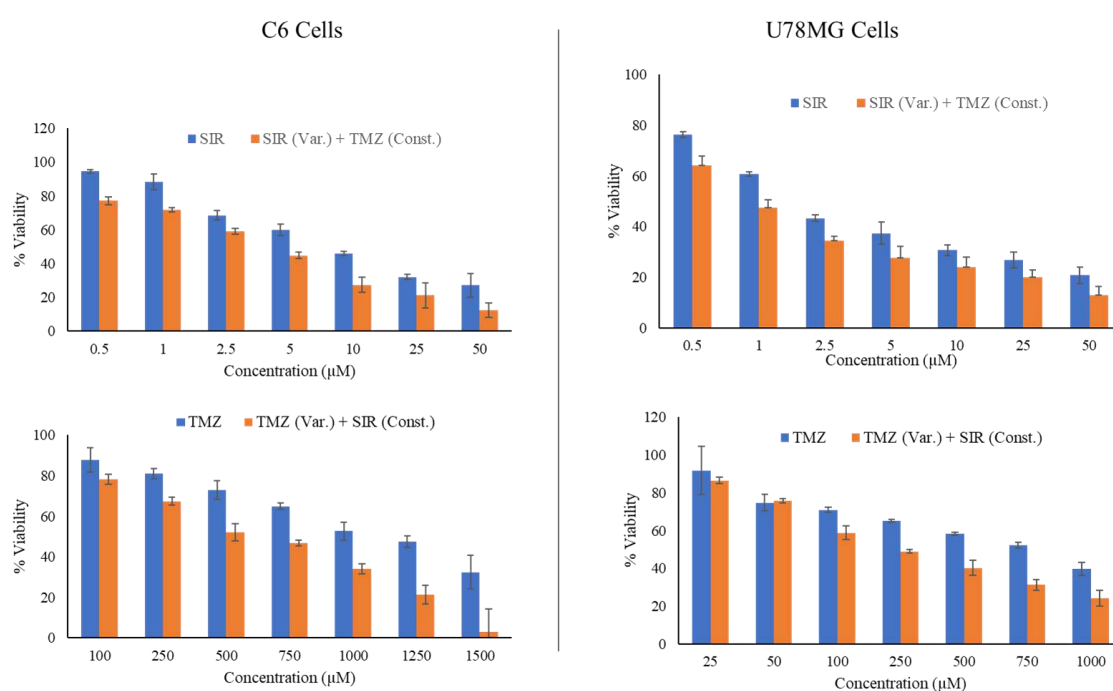


Figure 15. Combination index analysis for TMZ and sirolimus in C6 and U87 MG cells using cell cytotoxicity assay

Combination index for the TMZ and SIR was determined in C6 and U87MG glioma cells using Compusyn software (version 1.0). For the determination of multiple combinational approach were adopted including free TMZ, free SIR, TMZ constant SIR variable, and TMZ variable SIR constant. Using Chou-Talalay equation the obtained responses were evaluated and the combination index was determined.

Table 2. Combination index determination for TMZ and SIR in C6 and U87MG cells

C6 Cells				U87MG Cells			
TMZ (μM)	SIR (μM)	CI	Action	TMZ (μM)	SIR (μM)	CI	Action
1000	10	0.9	Synergism	500	2	0.75	Synergism
1250	10	0.47	Synergism	750	2	0.46	Synergism
1500	10	0.02	Strong synergism	1000	2	0.3	Strong synergism
1100	10	0.64	Synergism	800	2.5	0.67	Synergism
1100	25	0.74	Synergism	800	5	0.51	Synergism
1100	50	0.56	Synergism	800	10	0.6	Synergism
				800	25	0.79	Synergism
				800	50	0.45	Synergism

***In vivo* efficacy study**

The *in vivo* antitumor efficacy of developed hybrid nanoconjugates was evaluated in the C6-induced orthotropic glioma model in SD rats. Animals of different groups were treated with saline (negative control), positive control, free TMZ, free SIR, Hybrid TMZ NCs, non-targeted Hybrid TMZ NCs (SIR-loaded), and cRGD targeted hybrid TMZ NCs (SIR-loaded). The group treated with saline (positive control) showed mortality and died within 15 days after initiation of treatment, while the free TMZ and SIR-treated group showed mortality up to 40% and 60% respectively. Surprisingly, Hybrid TMZ-NCs, non-targeted Hybrid TMZ NCs, and cRGD targeted hybrid TMZ NCs showed no mortality with 100% survival after completion of treatment. Interestingly, a sudden weight loss was observed in all the animals after the injection of cells in the orthotropic site; later on, the animal started to show recovery in body weight except the positive control group, wherein the positive control animals showed no significant change in body weight till their death compared to other treated groups including free TMZ, free SIR, Hybrid TMZ NCs, non-targeted Hybrid TMZ NCs, and cRGD targeted hybrid TMZ NCs. Lastly, the brains of all treated groups were excised and evaluated for tumor growth, wherein brain weight and right-to-left hemispherical width (RH/LH) ratio were examined to confirm tumor growth. It was observed that the positive control group showed significantly higher brain weight and RH/LH ratio compared to the negative control, indicating the confirmation of the tumor model. TMZ and SIR-treated animals showed a

nominal reduction in brain weight and RH/LH ratio. At the same time, treatment with Hybrid TMZ NCs, non-targeted Hybrid TMZ NCs, and cRGD targeted hybrid TMZ NCs demonstrated a statistically significant decrease in the brain weight and the RH/LH width ratio, indicating better effectiveness *in vivo* than the free drugs treated group. For further confirmation, the excised brain was subjected to histopathological toxicity evaluation. Figure 16 shows the brain histopathological analysis of the positive control group with significantly higher infiltration of mononuclear cells at the site of injection (dotted line) depicting the tumor growth. In contrast, no such infiltration was observed in the left hemisphere of the brain, showing normal cellular morphology with no infiltration of C6 cells (uninjected site). Treatment with Hybrid TMZ NCs, non-targeted Hybrid TMZ NCs, and cRGD targeted hybrid TMZ NCs showed a reduction in the mononuclear cells in the right hemisphere of the brain compared to the positive control group, indicating their effectiveness on the tumor burden in glioma-induced rats.

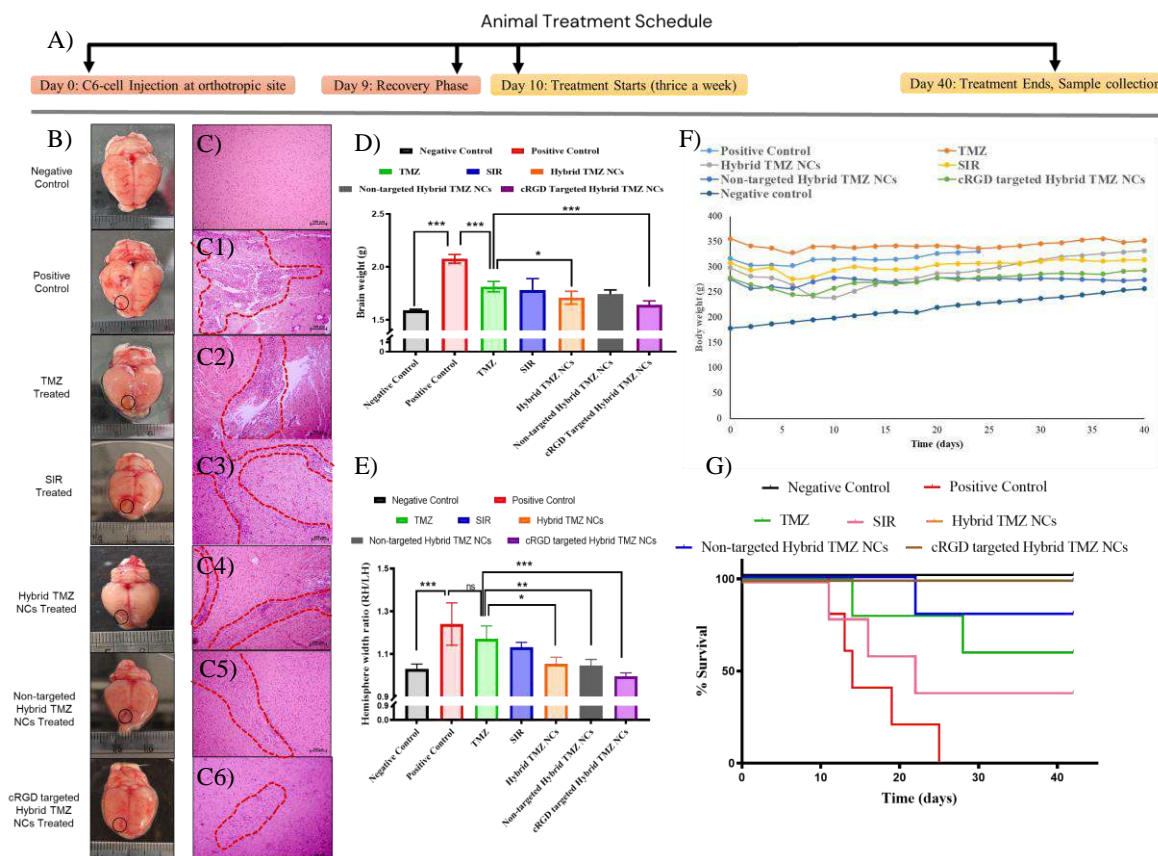


Figure 16. *In vivo* efficacy evaluation of hybrid nanoconjugates in C6-induced orthotropic glioma model in SD rats. A) Treatment schedule from the start of model development till the end of treatment. B) Representative brain images of treatment groups and its C-C6) brain histopathological evaluation of the right hemisphere (at the site of injection). D), E), F), and G) represent mean brain weight, hemispherical width ratio (RH/LH), body weight, and Kaplan-Meier survival plot of treated animals, respectively (scale bar: 100 μ m)

Histopathological Evaluation of hybrid nanoconjugates

The toxicity of the hybrid nanoconjugates in various organs, including the heart, lungs, liver, kidney, and spleen, were evaluated for histopathological modifications using H&E staining. The negative control (without tumor) group depicted normal morphology of the heart tissue with central nuclei and syncytial arrangement of fibers with intercalated disks. Similarly, treatment groups (positive control, free TMZ, free SIR, Hybrid TMZ NCs, non-targeted Hybrid TMZ NCs, and cRGD targeted Hybrid TMZ NCs) showed similar histology regarding fiber arrangement and the presence of intercalated discs. Lungs are considered to be highly perfused organs, becomes the primary target by the cancer cells, acquiring the sufficient nutrients and oxygen for the effective growth and survival. The positive control (tumor-bearing) group showed moderate tumor cell infiltration to the lungs with an increased mitotic nucleus of alveoli compared to the negative control group. Upon treatment with free TMZ and SIR, a slight reduction in infiltration/carcinoma growth was observed. Interestingly, treatment with Hybrid TMZ NCs, non-targeted Hybrid TMZ NCs, and cRGD targeted Hybrid TMZ NCs demonstrated no abnormalities of the carcinoma cells, especially in type 1, type 2, and the bronchioles with thickened alveolar septa, overall showing the positive anticancer outcome of the developed hybrid nanoconjugates on the lungs.

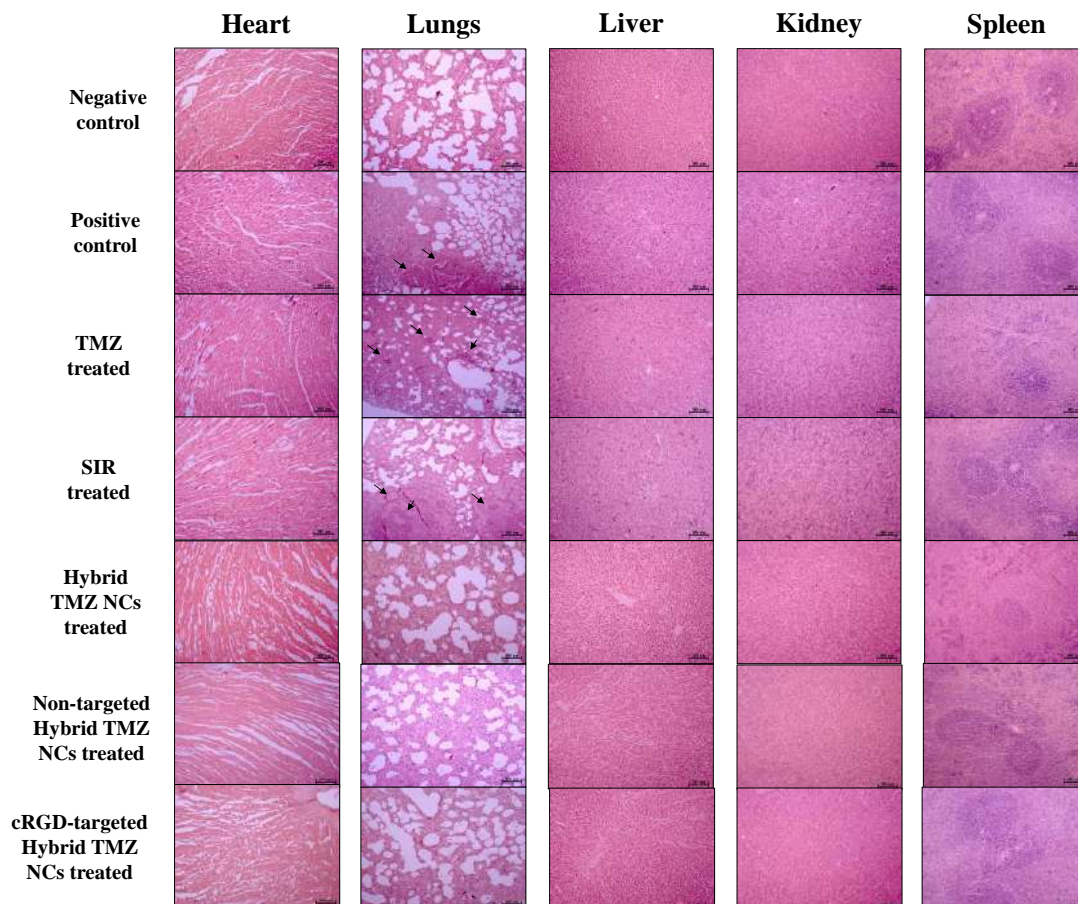


Figure 17. *In vivo* toxicity evaluation of hybrid nanoconjugate in majorly excised organs (heart, lungs, liver, kidney, and spleen) in C6-induced orthotopic glioma model in SD rats using H&E staining. (lungs: arrow indicates the presence of mitotic nucleus) (scale bar: 100 μ m)

Liver is the primary organ mainly responsible for the metabolism of various foreign substances, including proteins, carbohydrates, lipids, drugs, fats, etc. Therefore, evaluating the biocompatibility of the hybrid nanoconjugates in the liver is essential for the treatment perspective. The negative control group depicted the standard architecture of liver components composed of hepatocytes, central vein, Kupffer cells, bile duct cells, etc. In contrast, the positive control, TMZ and SIR-treated groups showed degenerative changes to the liver hepatocytes. In comparison, Hybrid TMZ NCs, non-targeted Hybrid TMZ NCs, and cRGD targeted Hybrid TMZ NCs treated groups demonstrated the biocompatibility behavior of the nanoconjugates resulting in the normal architecture of the liver components (hepatocytes, Kupffer cells, bile duct cells). However, the effectiveness of hybrid nanoconjugates was found to be inclined towards the healthy liver components nearly analogous to the negative control group. Kidney histology of the positive control tumor-bearing animals depicted alteration in the kidney components, such as atrophic renal tubules with increased peritubular space, and a similar trend was observed in free TMZ and SIR-treated animals. Treatment with Hybrid TMZ NCs, non-targeted Hybrid TMZ NCs, and cRGD targeted Hybrid TMZ NCs yielded improved kidney components with normal renal cortex, medulla, renal papilla, renal tubules, and glomerular tufts, demonstrating pathophysiology similar to the negative control group. The microscopic evaluation of splenic histology showed treatment with free TMZ, which showed moderate depletion in white pulp lymphoid components. At the same time cRGD targeted Hybrid TMZ NCs improved the splenic architecture with normal lymphoid follicles and sinuses with slight to minimal lymphoid depletion. Overall, the cRGD targeted hybrid nanoconjugates exhibited better biocompatibility and recuperated organ components to normal levels with minimal to negligible toxicity comparable to the negative control group.

Discussion

Temozolomide (TMZ) is considered as first line chemotherapeutic alkylating agent for the glioblastoma multiforme (GBM). The standard of care therapy for GBM includes surgical resection, followed by radiotherapy with adjuvant chemotherapy with Temozolomide. TMZ is marketed as Temodal® in the form of tablets, capsules, and injectables, given via oral and parenteral routes to the patients. It primarily shows its anticancer action by methylation of guanine and adenine sites of DNA, thereby causing cell death. TMZ has demonstrated potent antitumor activity. Still, it has several limitations, including a short half-life (~1.8-2 h), rapid

metabolism, quick clearance, pH-dependent degradation, less brain bioavailability, and dose-dependent toxicity, thereby restricting its therapeutic outcome.

Attempts have been made to overcome the TMZ-associated problems with numerous methods via encapsulation in various systems, including polymeric carrier, lipidic carrier, and inorganic strategies. For instance, Nordling-David et al. prepared TMZ-loaded PEGylated liposomes using a thin film hydration method yielding a small vesicle of *ca.* 121 nm and PDI <0.13 with an encapsulation efficiency of 23%. In-vivo, treatment demonstrated non-significant improvement in the survival rate compared to free TMZ [10]. Similarly, Duwa et al. prepared TMZ-loaded PLGA nanoparticles actively functionalized with cetuximab targeting EGFR receptors. Physiochemical characterization showed an average particle size of ~162 nm with a narrow PDI of 0.16 and encapsulation efficiency of 28.0% at drug loading of 1.4% w/w [11]. Despite encapsulation into the nanocarrier has improved the TMZ delivery, the unique physiochemical nature of the TMZ prevented the optimal encapsulation into the nanocarrier system. However, the conjugation-based approach could be utilized to overcome the TMZ-related concerns such as, loading capacity, encapsulation efficiency, TMZ stability, and toxicities. Likewise, a series of TMZ conjugated 2-methacryloyloxyethylphosphorylcholine (MPC) based polymer-drug conjugate was synthesized using RAFT polymerization, yielding the TMZ loading capacity ranging from 15-35 mol%. The resulting conjugate was used to prepare the nanoparticle with a particle size of 7-33 nm in range with improved half-life up to 19.1 h (~19 folds) compared to free TMZ [2]. In our current research work, a series of TMZ conjugated polymers were synthesized using a multistage reaction (Figure 1), describing the TMZ (**1**) was converted to its hydrazide derivative (**4**) in a three-step reaction as described. Simultaneously, amphiphilic block biocompatible polymer containing free COOH pendant (**7**) was synthesized using hydrogenation of mPEG-polycarbonate block polymer (**6**), followed by reaction with free NH₂ group of hydrazide derivative of TMZ to finally yield a series of polymer-drug conjugates, i.e, mPEG-b-P(CB-{g-COOH; g-TMZ₂₀}), mPEG-b-P(CB-{g-COOH; g-TMZ₄₀}), and mPEG-b-P(CB-{g-COOH; g-TMZ₆₀}) containing 20, 40, and 60 units of TMZ attached to the polymer backbone as a pendant group. Interestingly, the synthesized conjugates yielded nano-sized dispersions ranging from 90-510 nm with narrow PDI. The physiochemical characterization of obtained nanoconjugates demonstrated significantly improved loading capacity of TMZ up to 16.8%, 28.8%, and 38% w/w for mPEG-b-P(CB-{g-COOH; g-TMZ₂₀}), mPEG-b-P(CB-{g-COOH; g-TMZ₄₀}), and mPEG-b-P(CB-{g-COOH; g-TMZ₆₀}),

respectively of final polymer drug conjugate. Also, the loading capacity of TMZ attached to the polymer backbone was confirmed using UV-Vis spectrophotometry at λ_{max} 328 nm, and the obtained data were similar to the NMR spectroscopy.

The nanoconjugates of TMZ were prepared in various dispersive mediums (including pH 5.0, 6.0, and 7.4) and demonstrated varying particle sizes based on the units of TMZ units attached, wherein mPEG-b-P(CB-{g-COOH; g-TMZ₂₀}) demonstrated size ranging from 237.1 ± 6.48 to 323.7 ± 34.04 with PDI ranging from 0.387 ± 0.018 to 0.424 ± 0.043 , mPEG-b-P(CB-{g-COOH; g-TMZ₄₀}) showed an average particle size ranging from 90.9 ± 3.80 to 207.2 ± 8.37 with PDI of 0.099 ± 0.030 to 0.256 ± 0.011 ; while mPEG-b-P(CB-{g-COOH; g-TMZ₆₀}) exhibited an average particle size from 497.8 ± 6.56 to 552.0 ± 7.58 and PDI ranging from 0.218 ± 0.030 to 0.248 ± 0.013 . Although the nanoconjugates in various dispersive medium showed a good TMZ loading capacity of up to 38% w/w and a particle size of less than 510 nm, the size obtained using mPEG-b-P(CB-{g-COOH; g-TMZ₆₀}) was not suitable for the *in vitro* and *in vivo* therapeutics. Furthermore, mPEG-b-P(CB-{g-COOH; g-TMZ₂₀}) was excluded from the further studies as the loading capacity was significantly less, i.e., 16.8% w/w compared to 28.8% w/w for mPEG-b-P(CB-{g-COOH; g-TMZ₄₀}). Interestingly, mPEG-b-P(CB-{g-COOH; g-TMZ₄₀}) at physiological pH (7.4) showed good loading capacity and average particle size of 90.9 ± 3.80 and PDI of 0.256 ± 0.011 with a surface zeta potential of -12.06 ± 0.86 mV, was taken for further evaluation.

The stability of nanoconjugates in the biological environment is a key player in achieving an excellent therapeutic outcome. Accordingly, we have investigated colloidal and drug stability evaluation of mPEG-b-P(CB-{g-COOH; g-TMZ₄₀}) nanoconjugate under physiological conditions (37°C, pH 7.4). The colloidal stability assay at 37 °C showed a significant change in particle size from day 2, while no obvious change in particle size was observed at 4 °C with prolonged incubation up to 7 days. Simultaneously, the same samples were analysed at 37°C and pH 7.4 for the % TMZ content in intact form, wherein mPEG-b-P(CB-{g-COOH; g-TMZ₄₀}) showed a half-life of 5.88 h compared to 1.9 h for free TMZ. Despite the significant improvement in the loading capacity using the conjugation strategy, the stability perspective is still a concern to be taken care of. A similar outcome was observed by Patil et al., wherein conjugation of the molecule TMZ to the Poly(β -L-malic acid) yielded good loading efficiency of up to 17% w/w and slightly improved the stability half-life up to 6.25 h compared to 1.8 h of free TMZ [3]. In reported literature, preparation of a combinational mixture of two or more two components, i.e., hybrid nanoparticles, has elicited multiple

advantages, including improved drug stability, colloidal stability, biocompatibility, combinational drug delivery, ease in fabrication, controlled release properties, and reduced toxicities [12]. For instance, Tahir et al. prepared Lipid-polymer hybrid nanoparticles using PLGA polymer and DSPE-PEG lipid, yielding particle size ranging from 173-208 nm with excellent physical stability, biocompatibility, and a higher degree of internalization compared to free drug [13]. Similarly, Ebrahimian et al. prepared lipopolymeric nanoparticles using PLGA and PLGA-PC to enhance the stability of bromelain and facilitate oral delivery. The hybrid nanoparticles showed stable nanoparticles with no significant change in particle size, PDI, and zeta potential for over 1 month of storage [14]. Therefore, the preparation of hybrid component using mPEG-b-P(CB-{g-COOH; g-TMZ₄₀}) and mPEG-PLA using the thin film hydration method resulted in polymer-polymer hybrid nanoparticles (Hybrid TMZ-NCs) that showed a slightly higher average particle size of 105.7 ± 0.99 and PDI of 0.106 ± 0.033 , with a surface zeta potential of -6.79 ± 1.61 mV from -12.06 ± 0.86 mV of mPEG-b-P(CB-{g-COOH; g-TMZ₄₀}) alone. Furthermore, scanning electron microscopy (SEM) images confirmed uniform spherical shape particles with a slight increase in particle size compared to mPEG-b-P(CB-{g-COOH; g-TMZ₄₀}). Surprisingly, the colloidal and TMZ stability of the Hybrid TMZ-NCs nanoparticles was significantly improved for over 7 days and 120 h respectively, with half-life improved from 5.88 h to ~194 h. Besides, Hybrid TMZ-NCs exhibited more than 60% of TMZ in intact form after 120 h under physiological conditions, whereas no significant change was observed at 4°C. overall, *In vitro* evaluation of the nanoconjugates has demonstrated the marked enhancement of the physiochemical properties of the TMZ, wherein the stability and loading capacity of the TMZ was significantly improved using the above approach.

The evaluation of nanoconjugates was important regarding their intact pharmacological responses. Therefore, the Hybrid TMZ-NCs exhibited improved cellular uptake efficiency up to 74% and 79% in C6 and U87MG glioma cells that resulted in an IC₅₀ of Hybrid TMZ-NCs at ~645 and 866 μ M compared to 1125 and 738 μ M for free TMZ in C6 and U87MG glioma cells, respectively. The combination index was determined utilising the TMZ and SIR in various combinational approach to determine its synergism against the glioma cells. Wherein, in C6 and U87MG cells it was found that TMZ and SIR in 1500:10 μ M and 1000:2 μ M, respectively have demonstrated synergism, and could be potential candidate for further experiments. Moreover, the Hybrid TMZ-NCs demonstrated improved apoptosis rate up to 27.6% and 42.75% compared to 15.5% and 21.33% of free TMZ in C6

and U87MG glioma cells, respectively. Thereafter, a C6 cells induced orthotropic syngeneic glioma model was developed in rat brain. After the glioma model induction in rats, the change in physiological parameters, including right eye bulging, loss in body weight, reduced locomotion activity, etc., were observed to confirm the tumor growth. The animals were randomly divided and the treatment was initiated. After the completion of the treatment phase, animals were sacrificed, and change in brain parameters such as brain weight and hemispherical width ratio were noted. Wherein the Hybrid TMZ NCs, non-targeted Hybrid TMZ NCs, and cRGD targeted Hybrid TMZ NCs has resulted in a significant reduction in the brain weight, brain hemispherical width ratio (RH/LH), and the mononuclear cell infiltration in the brain tissue was observed compared to the positive control, i.e., effective towards the normal control group and eliciting the intact pharmacological response of the drug after conjugation and hybrid formulation. To understand the biocompatibility profile of the nanoconjugates, H&E staining was performed, showing the biocompatibility behaviour of the Hybrid TMZ-NCs component primarily because of the biomimetic mixture of the polycarbonate and polyester block polymer used. In all the majorly excised organs, including the heart, liver, kidney, and spleen, improvement or no toxicity was observed compared to the positive control and TMZ-treated animals. Especially in the lungs, mononuclear cell infiltration was observed, upon, treatment with Hybrid TMZ NCs, non-targeted Hybrid TMZ NCs, and cRGD targeted Hybrid TMZ NCs mononuclear cell infiltration was significantly reduced, demonstrating the effective antitumor response against the glioma cells. In previously reported literature, polycarbonate and polyester polymer are biocompatible and have been deployed in the biomedical field with diagnostic and therapeutic applications [15]. A similar observation has been seen by Rana et al., wherein no significant abnormalities were seen in major organs, including the brain, liver, heart, kidney, spleen, and lungs, and found to be safe post PEG-PLA polyester polymer administration [16]. Furthermore, He et al. prepared biodegradable polycarbonate micelles of diblock copolymer mPEG-b-PMCC for the anticancer agent delivery, depicting good biocompatibility with blood and all the major tissues as no such toxicity was observed in histopathological evaluation [17]. Furthermore, the presence of blood brain barrier (BBB) plays a vital role in segregating blood components and the brain microenvironment, thus making it more resistant to the permeation of drug molecules/carriers. However, cell penetrating peptides aids in transversing the molecules/carriers across the barrier with ease. Hence, cRGD peptide motif was attached to the hybrid system that enhances the BBB permeability[18]. Overall, the study demonstrated the conjugation and hybrid nanoformulation with peptide functionalisation approach

significantly improved the physiochemical and biological properties of the TMZ and SIR, especially the loading capacity, drug physiochemical drug stability, biocompatibility, and therapeutic effect compared to the free drug. Additionally, such a combination strategy could be explored for the targeted delivery of multiple drugs to target the multiple drug resistance pathways against glioma.

Conclusion

Although TMZ is a potent chemotherapeutic for the treatment of glioblastoma multiforme, still the therapeutic outcome is limited due to drug-related physiochemical limitations. However, the combination of conjugation and hybrid mixture approach has improved the loading capacity, stability half-life upto 194 h (>100 folds), and brain accumulation. The hybrid nanoconjugates have enhanced cellular uptake, IC₅₀, and apoptosis rate in C6 and U87MG glioma cells. Furthermore, in-vivo administration of peptide targeted and non-targeted has demonstrated improvement in the antitumor outcome compared to the free drug, with a significant reduction in the brain physical characteristics, i.e., brain weight, hemispherical width ratio, and improved the overall survival of rats. Histopathological evaluation has shown a reduction in the mononuclear cell infiltration in the brain tissue, and no other significant signs of toxicity were observed in the heart, liver, lungs, kidney, and spleen, demonstrating the biocompatibility of the developed hybrid nanoconjugates.

Impact of current Research

Glioblastoma (GBM) is the most prevalent and deadly primary malignant brain tumor in adults, accounting for 16% of all brain and central nervous system tumors. Conventional treatment primarily involves surgical resection, radiotherapy, and adjuvant temozolomide (TMZ) chemotherapy. TMZ is a second-generation imidazotetrazine DNA alkylating agent marketed as Temodal® in the form of capsules and injectables. TMZ being a potent molecule, it exhibits limitations, including development of resistance, short half-life, pH-dependent hydrolysis, and rapid clearance, resulting in <1% of the dose reaching the brain. Additionally, the studies have shown the direct involvement of the PI3K/Akt/mTOR/p53/autophagy pathway in the survival and progression of GBM. Still, the delivery of the molecule (autophagy inducer, rapamycin) to the target site of action is quite challenging, mainly due to drug-related (logp >5, high mol. wt) and physiological barriers

(tissue binding affinity, plasma binding, blood-to-plasma ratio, and blood-brain barrier (BBB)). Therefore, co-delivering autophagy inducer rapamycin and TMZ could help achieve multidimensional GBM treatment; however, the process is still problematic to achieve. Herein, we propose to design and synthesize a carrier system that can co-deliver hard-to-deliver molecules rapamycin and TMZ to the targeted site of action, *viz.*, transversing the BBB.

In the current research, we prepared a cRGD peptide-functionalized polymer-polymer hybrid system using polycarbonate TMZ polymer conjugate and polyester mPEG-PLA polymer coloaded with rapamycin against GBM. With this hybrid surface functionalisation approach, the delivery and molecules related problems associated to variety of drugs could be addressed with a broad range from highly hydrophilic to hydrophobic molecules, which is itself a promising technology. This actively functionalised hybrid system can overcome the limitations associated to the potential molecules for the treatment of various cancer *viz.* improving stability, systemic circulation, tissue permeability, targeted delivery, with reduced clearance, toxicities, resistance burden. Thus, it could be the potential candidate for reducing the clinically delivery related limitations across the blood brain barrier and needed to be explored in more detail for evaluating it against the broad range of complications/diseases for better patient compliance.

References

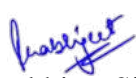
- [1] R. Jatyán, P. Singh, D.K. Sahel, Y.G. Karthik, A. Mittal, D. Chitkara, Polymeric and small molecule-conjugates of temozolomide as improved therapeutic agents for glioblastoma multiforme, *J. Control. Release.* 350 (2022) 494–513. <https://doi.org/https://doi.org/10.1016/j.jconrel.2022.08.024>.
- [2] S.M. Ward, M. Skinner, B. Saha, T. Emrick, Polymer–Temozolomide Conjugates as Therapeutics for Treating Glioblastoma, *Mol. Pharm.* 15 (2018) 5263–5276. <https://doi.org/10.1021/acs.molpharmaceut.8b00766>.
- [3] R. Patil, J. Portilla-Arias, H. Ding, S. Inoue, B. Konda, J. Hu, K.A. Wawrowsky, P.K. Shin, K.L. Black, E. Holler, J.Y. Ljubimova, Temozolomide Delivery to Tumor Cells by a Multifunctional Nano Vehicle Based on Poly(β -L-malic acid), *Pharm. Res.* 27 (2010) 2317–2329. <https://doi.org/10.1007/s11095-010-0091-0>.
- [4] R. Scopel, M.A. Falcão, A.R. Cappellari, F.B. Morrone, S.S. Guterres, E. Cassel, A.M. Kasko, R.M.F. Vargas, Lipid-polymer hybrid nanoparticles as a targeted drug delivery system for melanoma treatment, *Int. J. Polym. Mater. Polym. Biomater.* 71 (2022) 127–138. <https://doi.org/10.1080/00914037.2020.1809406>.
- [5] S.S. Pukale, S. Sharma, M. Dalela, A. kumar Singh, S. Mohanty, A. Mittal, D. Chitkara, Multi-component clobetasol-loaded monolithic lipid-polymer hybrid nanoparticles ameliorate imiquimod-induced psoriasis-like skin inflammation in Swiss albino mice, *Acta Biomater.* 115 (2020) 393–409.

<https://doi.org/https://doi.org/10.1016/j.actbio.2020.08.020>.

- [6] R. Jatyán, D.K. Sahel, P. Singh, R. Sakhuja, A. Mittal, D. Chitkara, Temozolomide-fatty acid conjugates for glioblastoma multiforme: In vitro and in vivo evaluation., *J. Control. Release.* 23 (2023) S0168-3659. <https://doi.org/10.1016/j.jconrel.2023.05.012>.
- [7] S. Sharma, S. Pukale, D.K. Sahel, P. Singh, A. Mittal, D. Chitkara, Folate targeted hybrid lipopolymeric nanoplexes containing docetaxel and miRNA-34a for breast cancer treatment, *Mater. Sci. Eng. C.* 128 (2021) 112305. <https://doi.org/https://doi.org/10.1016/j.msec.2021.112305>.
- [8] A. Mittal, D. Chitkara, S.W. Behrman, R.I. Mahato, Efficacy of gemcitabine conjugated and miRNA-205 complexed micelles for treatment of advanced pancreatic cancer, *Biomaterials.* 35 (2014) 7077–7087. <https://doi.org/https://doi.org/10.1016/j.biomaterials.2014.04.053>.
- [9] S. Sharma, S. Mazumdar, K.S. Italiya, T. Date, R.I. Mahato, A. Mittal, D. Chitkara, Cholesterol and Morpholine Grafted Cationic Amphiphilic Copolymers for miRNA-34a Delivery, *Mol. Pharm.* 15 (2018) 2391–2402. <https://doi.org/10.1021/acs.molpharmaceut.8b00228>.
- [10] M.M. Nordling-David, R. Yaffe, D. Guez, H. Meirou, D. Last, E. Grad, S. Salomon, S. Sharabi, Y. Levi-Kalishman, G. Golomb, Y. Mardor, Liposomal temozolomide drug delivery using convection enhanced delivery, *J. Control. Release.* 261 (2017) 138–146. <https://doi.org/https://doi.org/10.1016/j.jconrel.2017.06.028>.
- [11] R. Duwa, A. Banstola, F. Emami, J.-H. Jeong, S. Lee, S. Yook, Cetuximab conjugated temozolomide-loaded poly (lactic-co-glycolic acid) nanoparticles for targeted nanomedicine in EGFR overexpressing cancer cells, *J. Drug Deliv. Sci. Technol.* 60 (2020) 101928. <https://doi.org/https://doi.org/10.1016/j.jddst.2020.101928>.
- [12] S. Tan, X. Li, Y. Guo, Z. Zhang, Lipid-enveloped hybrid nanoparticles for drug delivery, *Nanoscale.* 5 (2013) 860–872. <https://doi.org/10.1039/C2NR32880A>.
- [13] N. Tahir, A. Madni, A. Correia, M. Rehman, V. Balasubramanian, M.M. Khan, H.A. Santos, Lipid-polymer hybrid nanoparticles for controlled delivery of hydrophilic and lipophilic doxorubicin for breast cancer therapy, *Int. J. Nanomedicine.* 14 (2019) 4961–4974. <https://doi.org/10.2147/IJN.S209325>.
- [14] M. Ebrahimian, F. Mahvelati, B. Malaekhe-Nikouei, E. Hashemi, F. Oroojalian, M. Hashemi, Bromelain Loaded Lipid-Polymer Hybrid Nanoparticles for Oral Delivery: Formulation and Characterization, *Appl. Biochem. Biotechnol.* 194 (2022) 3733–3748. <https://doi.org/10.1007/s12010-022-03812-z>.
- [15] I. Ansari, P. Singh, A. Mittal, R.I. Mahato, D. Chitkara, 2,2-Bis(hydroxymethyl) propionic acid based cyclic carbonate monomers and their (co)polymers as advanced materials for biomedical applications, *Biomaterials.* 275 (2021) 120953. <https://doi.org/https://doi.org/10.1016/j.biomaterials.2021.120953>.
- [16] S. Rana, J. Singh, A. Wadhawan, A. Khanna, G. Singh, M. Chatterjee, Evaluation of In Vivo toxicity of Novel Biosurfactant from *Candida parapsilosis* loaded in PLA-PEG Polymeric Nanoparticles, *J. Pharm. Sci.* 110 (2021) 1727–1738. <https://doi.org/https://doi.org/10.1016/j.xphs.2021.01.004>.
- [17] M. He, R. Wang, P. Wan, H. Wang, Y. Cheng, P. Miao, Z. Wei, X. Leng, Y. Li, J. Du, J. Fan, W. Sun, X. Peng, Biodegradable Ru-Containing Polycarbonate Micelles for Photoinduced Anticancer Multitherapeutic Agent Delivery and Phototherapy Enhancement, *Biomacromolecules.* 23 (2022) 1733–1744. <https://doi.org/10.1021/acs.biomac.1c01651>.
- [18] Y. Miura, T. Takenaka, K. Toh, S. Wu, H. Nishihara, M.R. Kano, Y. Ino, T. Nomoto, Y. Matsumoto, H. Koyama, H. Cabral, N. Nishiyama, K. Kataoka, Cyclic RGD-Linked Polymeric Micelles for Targeted Delivery of Platinum Anticancer Drugs to Glioblastoma through the Blood–Brain Tumor Barrier, *ACS Nano.* 7 (2013) 8583–8592. <https://doi.org/10.1021/nn402662d>.

Date: 31/08/2023

Place: Pilani


Prabhjeet Singh
(Ph.D. Research Scholar)